



Adaptation of fen peatlands to climate change: rewetting and management shift can reduce greenhouse gas emissions and offset climate warming effects

Carla Bockermann · Tim Eickenscheidt ·
Matthias Drösler

Received: 24 May 2023 / Accepted: 17 December 2023
© The Author(s) 2024

Abstract In Germany, emissions from drained organic soils contributed approximately 53.7 Mio. t of carbon dioxide equivalents (CO₂-eq) to the total national greenhouse gas (GHG) emissions in 2021. In addition to restoration measures, shifting management practices, rewetting, or using peatlands for paludiculture is expected to significantly reduce GHG emissions. The effects of climate change on these mitigation measures remains to be tested. In a 2017 experimental field study on agriculturally used grassland on organic soil, we assessed the effects of rewetting and of predicted climate warming on intensive grassland and on extensively managed sedge grassland (transplanted *Carex acutiformis* monoliths). The testing conditions of the two grassland types included drained versus rewetted conditions (annual mean water table of −0.13 m below soil surface), ambient versus warming conditions (annual mean air

temperature increase of +0.8 to 1.3 °C; use of open top chambers), and the combination of rewetting and warming. We measured net ecosystem exchange of CO₂, methane and nitrous oxide using the closed dynamic and static chamber method. Here, we report the results on the initial year of GHG measurements after transplanting adult *Carex* soil monoliths, including the controlled increase in water level and temperature. We observed higher N₂O emissions than anticipated in all treatments. This was especially unexpected for the rewetted intensive grasslands and the *Carex* treatments, but largely attributable to the onset of rewetting coinciding with freeze–thaw cycles. However, this does not affect the overall outcomes on mitigation and adaptation trends. We found that warmer conditions increased total GHG emissions of the drained intensive grassland system from 48.4 to 66.9 t CO₂-eq ha^{−1} year^{−1}. The shift in grassland management towards *Carex* paludiculture resulted in the largest GHG reduction, producing a net cooling effect with an uptake of 11.1 t CO₂-eq ha^{−1} year^{−1}. Surprisingly, we found that this strong sink could be maintained under the simulated warming conditions ensuing an emission reduction potential of −80 t CO₂-eq ha^{−1} year^{−1}. We emphasize that the results reflect a single initial measurement year and do not imply the permanence of the observed GHG sink function over time. Our findings affirm that rewetted peatlands with adapted plant species could sustain GHG mitigation and potentially promote ecosystem resilience, even under climate warming. In a

Responsible Editor: Klaus Butterbach-Bahl

Supplementary Information The online version contains supplementary material available at <https://doi.org/10.1007/s10533-023-01113-z>.

C. Bockermann (✉) · T. Eickenscheidt · M. Drösler
Peatland Science Center, University of Applied Sciences
Weihenstephan-Triesdorf, Freising, Germany
e-mail: carla.bockermann@hswt.de

C. Bockermann
Technical University of Munich, Chair of Atmospheric
Environmental Research, Freising, Germany

warmer world, adaptation measures for organic soils should therefore include a change in management towards paludiculture. Multi-year studies are needed to support the findings of our one-year experiment. In general, the timing of rewetting should be considered carefully in mitigation measures.

Keywords *Carex* · GHG mitigation · Grassland · Nature-based solution · Organic soils · Paludiculture

Introduction

Peatlands are globally under pressure from human alterations and climate change. In the last century human-induced alterations (e.g., drainage, intensive agricultural use, eutrophication, peat extraction) have disturbed peatland carbon (C) and nitrogen (N) cycles on a global scale and turned peatlands into “hot-spots” of greenhouse gas (GHG) emissions (cf. Drösler et al. 2008; Tiemeyer et al. 2016, 2020; Tanneberger et al. 2021). Regulating the high emission potential that is attributable to the substantial amounts of C and N stored in these organic soils will depend on how we use peatlands in the future. In Germany, organic soils cover 1.93 Mio ha or 5.4% of the total land area (Wittnebel et al. 2023). About 92% are currently drained and mostly used as grassland and arable land (Tiemeyer et al. 2020). Emissions from organic soils amounted to approximately 53.7 Mio t CO₂-equivalents (CO₂-eq) or 7.0% of the total national GHG emissions in 2021 (UBA 2023: NIR 2023 Germany). As Germany aims at reducing national GHG emissions by 65% (compared with 1990) by 2030 (BMEL 2020), the high emissions from peat soils drained for agriculture make them a sensible target for largescale mitigation efforts. Yet, halting all GHG emissions will not prevent the climate impacts that are already occurring, making climate change adaptation imperative (IPCC 2018; Loisel and Gallego-Sala 2022). The EU proclaims a high political ambition in the goal to become climate resilient by 2050 as stated in the 2021 EU strategy on adaptation to climate change (EC 2021). Strategic emphasis on nature-based solutions for adaptation promoting the protection and restoration of peatlands

highlights the need to fill gaps in data and methodologies on climate change adaptation, risk, vulnerability and resilience.

Climate change affects organic soils through altered temperature and moisture regimes (e.g., Hamidov et al. 2018; Laine et al. 2019; IPCC 2021; Loisel et al. 2021; Fan et al. 2022). According to the Intergovernmental Panel on Climate Change (IPCC), the global mean land surface air temperature has increased by 1.6 °C from 1850–1900 to 2011–2020 (IPCC 2021). Since 1950, human-induced climate change has led to increases in frequency and longevity of drought periods together with heavy rainfall events in most regions of the world. Anticipated impacts of climate change include alterations of key water cycle characteristics such as regional shifts in precipitation pattern, increased evapotranspiration, and decreased soil water availability. Focusing on peatlands, substantial evidence exists about temperature and groundwater level being the key factors controlling peat decomposition rates and therefore influencing CO₂, CH₄ and N₂O exchange between the ecosystem and the atmosphere (e.g., Jungkunst et al. 2008; Pearson et al. 2015; Laine et al. 2019; Günther et al. 2020; Offermanns et al. 2023). For the temperate zone, it is assumed that the predicted temperature increase will accelerate peat decay (e.g. Glatzel et al. 2006) and will further enhance CO₂ and N₂O emissions from drained peatlands, causing a positive feedback on climate warming (Loisel et al. 2021). In agriculturally used peatlands, groundwater level is often found to be the most important regulating factor for GHG emissions as it defines the boundaries of oxic and anoxic soil layers (Evans et al. 2021). Besides temperature and water table, the predominant plant community regulates CH₄ fluxes (Turetsky et al. 2014) while fertilizer application enhances N₂O fluxes (Leppelt et al. 2014; Eickenscheidt et al. 2014).

The study region in southern Bavaria has experienced an increase of mean annual air temperature of 2.0 °C and changed precipitation pattern between 1951 and 2019, with intensified heavy rainfall events in the spring and decreased summer precipitation (LfU 2021). Regional climate models project a mean temperature change of between +1.0 (+0.8 to +1.4) °C under IPCC emission scenario RCP2.6 (RCP = Representative Concentration Pathway) and

up to +1.5 (+0.8 to +2.2) °C under RCP8.5 for the period 2021–2050 compared to the 30-year mean of the reference period 1971–2000 for southern lowland Bavaria (LfU 2021). The expected climatic changes are likely to exacerbate summer droughts, winter and spring flooding, and entail longer vegetation periods. While prolonged growing seasons potentially result in enhanced plant biomass production and consequently CO₂ uptake, higher evapotranspiration rates may lead to further groundwater level drawdown of drained areas (Huang et al. 2021; IPCC 2021; Wunsch et al. 2022). Depending on the prevalent plant communities and the agricultural management, biomass yield and GHG emissions may thus increase or decrease in a changing climate (Shaver et al. 2000).

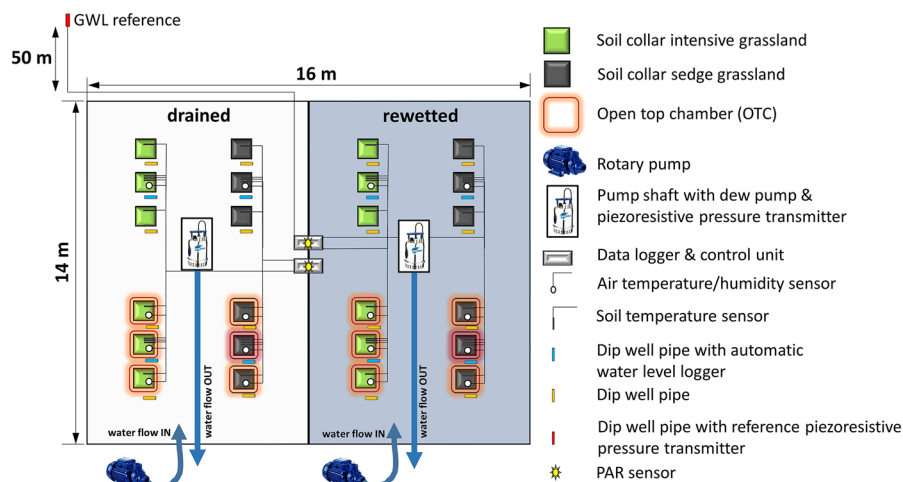
Different strategies for drained organic soils are currently discussed and practiced to achieve a reduction in peat mineralization, mitigate GHG emissions, and adapt systems to changing environmental conditions (e.g. partial rewetting, management extensification, paludiculture, restoration). Active adaptation can lead to a recovery of important ecosystem functions, increasing peatland resilience to adverse impacts of climate change (Renou-Wilson et al. 2014; Loisel and Gallego-Sala 2022). Rewetting is the general mitigation measure suggested by the IPCC Wetlands Supplement (IPCC 2014) for degraded peatlands and is deemed a suitable nature-based solution for GHG reduction (Evans et al. 2021; Tanneberger et al. 2021; IPCC 2022). While peatland restoration can successfully mitigate GHG emissions, paludiculture (Latin ‘*palus*’ = swamp) can serve both reduced GHG emissions as well as continued biomass production (Abel et al. 2013; Tanneberger et al. 2022).

While rewetting and paludiculture are increasingly being tested on degraded organic soils (Günther et al. 2014; Minke et al. 2016; Wilson et al. 2016; Kandel et al. 2019; Lahtinen et al. 2022), the response of paludiculture to climate change has been rarely considered in field research (Gong et al. 2020; BMUV 2021 (National Peatland Protection Strategy 2021); Freeman et al. 2022; Loisel and Gallego-Sala 2022). Several incubation studies investigated peatland emission responses to rewetting combined with temperature increase (e.g., Updegraff et al. 2001; Estop-Aragónés and Blodau 2012; Salimi et al. 2021), but most studies question the transferability to field condition. Further, the mentioned studies report differing

responses of GHG fluxes to warming in the various ecosystems. Warming experiments in situ mostly focus on boreal or subarctic regions, which are most susceptible to climate change, and simulate the anticipated water level drawdown (cf. Pearson et al. 2015; Gong et al. 2020). Model simulations have given insights into feedbacks of water table and temperature increase (i.e., climate change scenarios) on peat. Nugent et al. (2019) argue for active restoration in post peat extraction sites beyond just rewetting to accomplish the greatest mitigation success. Günther et al. (2020) recently combined climate change scenarios with peatland rewetting. Model predictions are in support of this mitigation approach and the researchers argue for an immediate rewetting of all drained peatlands. In the field, simulating climate change is complex, while inducing the presumable key feature—temperature increase—can easily be accomplished by passively trapping solar radiation using open top chambers (OTCs) (Marion et al. 1997). The only field study on warming effects on GHGs in rewetted peatlands so far was conducted in *Sphagnum*-dominated bogs by Oestmann et al. (2022; *Sphagnum* farm). They reported increased CO₂ and CH₄ emissions under warmer conditions (especially in the presence of vascular plants) while N₂O was negligible and emphasized the need for high water levels.

To our knowledge, field observations on the response of drained fen grassland to mitigation measures are scarce and no empirical evidence exists on whether beneficial effects persist under climate change. We set out to answer the guiding question of whether rewetted peatlands with adapted plant species (paludiculture) can sustain GHG mitigation under climate warming. Therefore, we conducted a full factorial field manipulation experiment on previously drained fen grassland where we compared fertilized sweetgrass versus unfertilized sedge (*Carex acutiformis*) under drained versus rewetted conditions, and additionally under ambient temperature versus warming conditions (resulting in eight treatments). Our objectives were to quantify the effects of the manipulations on GHG exchange (CO₂, CH₄ and N₂O) and on biomass yield to assess mitigation potentials for different management strategies of grassland on organic soils.

Fig. 1 Schematic setup of the experimental field with intensive vs. sedge grassland (*Carex acutiformis*) in the Freisinger Moos. In two adjacent basins, the water table was actively manipulated: drained conditions on the left (reproduction of the surrounding field GWL) and rewetted conditions on the right (surrounding field GWL + 0.2–0.3 m). Treatments in the lower half were subjected to passive warming (open top chambers)



Methods

Study site

We conducted the field experiments in a drained fen peatland, the Freisinger Moos, at the northern boundary of the Munich gravel plain, about 30 km north of Munich, Germany (experimental site at 48°22'N, 11°41'E; elevation 453 m a.m.s.l.). The systematic drainage and cultivation of this groundwater-fed fen complex started in 1914 and approximately 88.8% of the peatland area (total area 1606 ha) is currently used for agriculture (about 24.1% cropland, 23.5% intensive grassland, and 41.2% extensive grassland) (Eberl 2016). Intensive grassland management is defined as at least two harvests per year and subsequent fertilization, extensive grassland management as one harvest per year and no fertilization. The Freisinger Moos lies within the cool temperate zone characterized by humid continental climate (Köppen-Geiger climate classification). According to the German weather service (DWD) climate station at the Munich airport located 10 km east of the study area (station at 48°21'N, 11°48'E; elevation 446 m a.m.s.l.), mean annual air temperature was 9.2 °C and mean annual total precipitation was 759 mm in the time period 1993–2022 (DWD 2023).

We selected an intensively managed grassland near a drainage ditch for the setup of our experimental treatments. The original drained grassland vegetation consisted mainly of *Lolium perenne*, *Phleum pratense*, *Poa pratensis*, *Festuca pratensis*, and

Alopecurus pratensis (hereafter referred to as 'intensive grassland' or abbreviated as 'I') with an average groundwater table of approximately –0.4 m (considered as 'drained' or abbr. 'D'). We classified the soil type of the study area as sapric histosol (IUSS Working Group WRB 2015). The soil had a 2.5–3 m peat layer comprised of decomposing sedges, reeds, and alder. The top layers were characterized by about 30 cm highly earthified peat with an organic C content of 34% (C_{org}), total N content of 2.43%, a bulk density between 0.22 and 0.33 g cm⁻³, pH (CaCl₂) of 6.5 (0–10 cm) and 5.9 (10–30), and degradation stage H9. The underlying peat layers had 45 to 48% C_{org} , and degradation stages H2 to H5. We emphasize that this soil characterization applies to the original field conditions before manipulation.

Experimental design

We set up a full factorial field design in 2016 to examine the effects of land use change (shift from intensively managed grassland, abbreviated as 'I', toward management extensification with plant community shift dominated by the sedge *Carex acutiformis* Ehrh., no fertilizer, hereafter referred to as 'Carex grassland' or abbreviated as 'C'), increased temperature ('ambient temperature' abbreviated as 'A' vs. passive warming with open top chambers, OTCs, abbreviated as 'W'), and increased groundwater level (GWL; reference water level hereafter referred to as 'drained' abbreviated as 'D' vs. rewetting via controlled automatic pumping abbreviated as 'R') in 2017 (overview

see Fig. 1 and Table 1). Within the original intensively managed grassland field, we established two zones for *Carex* grassland on 07 June 2016, six months prior to the measurement start, to allow for an adaptation period of the adult *Carex* stand to the new site conditions. The *Carex* grassland plots were established by transplanting *C. acutiformis* soil monoliths (1 m² per spatial replicate (plot), consisting of four undisturbed 50×50×30 cm sub blocks) from nearby extensively managed grassland fields under similar drainage conditions. The depth of 30 cm was chosen as the largest portion of root and rhizome biomass was found within 0–30 cm at the donor site. To account for the potential effect of soil disturbance by transplanting the *Carex* monoliths, we simulated this effect in the intensive grassland zones by cutting and lifting 50×50×30 cm sub blocks as well. We cut the vegetation of all treatments in mid-October 2016 to simulate the autumn harvest (cut at about 10 cm above the surface).

Two adjacent basins were constructed in the experimental field using sheet piles driven 2.3 m into the peat soil layer to simulate percolation fen conditions with slow subsurface water flow above the mineral soil layer, and with wall heights of 20 cm above the surface to prevent the surface flow of water and nutrients between the two basins. We installed networks of drainage tubes and central pump shafts to create a reference GWL basin and a basin with an increased GWL, each 8×14 m comprising intensive (=I) and extensive *C. acutiformis* (=C) grassland. Inside the reference basin (D=drained), we exactly reproduced the GWL of the adjacent drained grassland via a programmable controlling unit (DT85, dataTaker) and two dip well pipes, each equipped with a piezoresistive pressure transmitter (PR-26W, KELLER AG,

CH). One of these dip well pipes was installed approx. 50 m outside the basins and served as reference for the adjacent drained grassland GWL, whereas the other was located in the central pump shaft of the reference basin. In addition, a third piezoresistive pressure transmitter was installed in the central pump shaft of the second basin to control the water level increase compared to the reference basin. As the GWL was controlled in the basin center, a small slope in the surface terrain toward the I treatments resulted in slightly higher GWL (i.e., water table closer to the surface) in the ID and CD treatments. The GWL in the increased water table basin (R=rewetted) was set to a dynamic difference of 0.2–0.3 m above the reference value to give an annual mean GWL of around 0.1 m below the surface (max of 0.03 m above the surface) for wet cultivation conditions (paludiculture). The water tables were automatically adjusted to the respective levels with a ± 1 cm hysteresis at 5-s intervals by pumping water from a drainage ditch into (rotary pump, see Fig. 1) or out of (dew pump) each basin (note: water table manipulation system started operating on 07 February 2017 due to power supply problems). We allowed the rewetted basin GWL to mirror fluctuations of the reference GWL in a similar, but dampened magnitude. The chemistry of the rewetting water supplied by the adjacent drainage ditch revealed a moderate nutrient load (see Supplementary Table S1 for water chemistry analysis).

We permanently installed soil collars (PVC, inside dimensions 75×75 cm, blade depth 10 cm) for chamber GHG flux measurements with three spatial replicates (plots) for each of the eight designated treatments. The distance between ambient vs. warming treatments was 2.5 m and between fertilized vs. unfertilized treatments 3.5 m. All plots were equipped with

Table 1 Overview of the eight grassland treatments with the respective management events, water level and temperature conditions

Grassland type	Harvest	Fertilization	Water level	Temperature	Abbreviation
intensive grassland (<i>Lolium perenne</i> , <i>Phleum pratense</i> , <i>Poa pratensis</i> , <i>Festuca pratensis</i> , <i>Alopecurus pratensis</i>)	2: 19.06. and 28.09.2017	2×25 m ³ cattle slurry ha ⁻¹ ; 2017 total: 160.0 kg N _{tot} ha ⁻¹ year ⁻¹	Drained	Ambient	IDA
				Warming	IDW
			Rewetted	Ambient	IRA
				Warming	IRW
<i>Carex</i> dominated grassland (> 90% <i>Carex acutiformis</i>)	1: 28.09.2017	no	Drained	Ambient	CDA
				Warming	CDW
			Rewetted	Ambient	CRA
				Warming	CRW

sensors for soil temperature measurements at -2 cm (ST2) (SKTS200, Skye Instruments, UK) and adjacent PVC dip well pipes (6 cm diameter, 1 m length, Brunnenfilter DN 50, 2") for GWL measurements with one automatic water level logger per treatment (Rugged TROLL 100, In-Situ Inc., US). The central plots of the ambient air temperature treatments and all three plots of the temperature manipulation treatments were additionally equipped with air temperature sensors at 20 cm (Tair) (HC2-S3 sensors with non-ventilated radiation shields AC1000, Rotronic AG, Switzerland). The central plots of all treatments were further equipped with soil temperature sensors at -5 (ST5) and -10 (ST10) cm depths. Two photosynthetically active radiation (PAR) sensors (BF2H, Delta-T Devices Ltd, UK) were installed at 2 m height centrally in the experimental area. Air temperature at 2 m and air pressure were measured within 20-m proximity of the test site. PAR values were logged as 30-min averages of 1-min measurements while all other values were measured and logged in 30-min intervals (DL2e data logger, Delta-T Devices Ltd, UK). The use of boardwalks prevented artificial soil movement and resulting gas fluxes.

In treatments for temperature manipulation (W=warming, A=ambient temperature), we permanently installed UV-permeable acrylic open-top chambers (OTCs; Ps-plastic Kunststoff GmbH, Germany) of 50 cm height mounted on 5 cm feet to allow for wind circulation inside the OTCs. The open top was of equal size as the basal area (soil collars). We used UV-permeable acrylic extensions (50 cm height) when the vegetation stand exceeded 50 cm in height. In case of GHG measurements or harvesting, the OTCs were temporarily removed for the duration of the activity.

Vegetation development and yield

During the measurement period in 2017, we harvested all intensive grassland treatments on 19 June and 28 September (cut at about 10 cm above the surface) with subsequent organic fertilizer application (total 2017: 50 m^3 cattle slurry $\text{ha}^{-1} = 1242.5 \text{ kg C}_{\text{org}} \text{ ha}^{-1} \text{ year}^{-1}$ and $160.0 \text{ kg N}_{\text{tot}} \text{ ha}^{-1} \text{ year}^{-1}$; application inside the plots only) according to the agricultural practice of the adjacent intensive grassland. Fertilizer samples were analyzed for C_{org} and total nitrogen (N_{tot}) concentrations via wet and dry

combustion respectively (AGROLAB GmbH, Germany). On 25 April 2017, when vegetation was still low (approx. 20 cm), single sweetgrass plants were removed from all *Carex* treatments to maintain at least 90% *C. acutiformis* cover in the measurement area. The weeded biomass was not included in the export as the total removed sweetgrass biomass was low and no effect on GPP was detected (see Fig. 3). This may result in a slight underestimation of the total C export. We harvested all biomass once on 28 September (cut at about 10 cm above the surface) and no fertilizer was applied, adhering to local management regimes for extensive grasslands nearby. The harvested biomass was oven dried at 60°C for 48 h to determine the dry matter (DM) weight per plot for yield calculations. Milled (0.5 mm) mixed subsamples per treatment were analyzed via dry combustion (AGROLAB GmbH, Germany) to determine the C_{tot} concentrations.

CO₂ gas flux measurements, calculation, and modelling

We determined CO₂ fluxes triweekly (weather dependent) from December 2016 to January 2018 to get sufficient coverage of the annual spectra of temperature, radiation, and vegetation development phases. Additional measurements were done in case of harvest events. To capture the full daily ranges of photosynthetically active radiation (PAR), and soil and air temperature, CO₂ flux measurements started 1 h before sunrise (time of $\text{PAR} = 0$ and min. temperatures) and ended midafternoon (time of max. soil temperatures). Until noon (max. PAR), we alternated ecosystem respiration (R_{eco}) measurements using opaque chambers (PVC) and net ecosystem exchange (NEE) measurements using transparent chambers (acrylic glass, PAR attenuation 5%) (dimensions $78 \times 78 \times 51$ cm; PS Plastics, Germany). Over closure times between 90–120 s for NEE measurements (transparent chambers) and 120–300 s for R_{eco} measurements (opaque chambers) the chambers were connected to an infrared gas analyser (IRGA; LI-840, LI-COR, USA) in a closed loop to measure CO₂ and H₂O concentrations of the mixed chamber air instantaneously (continuously operating fans). Water vapor detection is relevant to correct the measured CO₂ concentration accounting for dilution effects in the gas

mixture where dissolved CO₂ in water can cause underestimation of actual CO₂ mole fractions (e.g. Pérez-Priego et al. 2015), and further to account for spectral cross-sensitivity in infrared radiation absorption of CO₂ and H₂O molecules (IRGA-specific) potentially leading to an overestimation of CO₂. Gas concentration data were logged every 5 s (GP2 Data logger, Delta-T Devices, UK). A more detailed description of the chamber design and the measurement procedure is given by Drösler (2005) and Eickenscheidt (2015). Chamber air temperature was logged every 5 s over the chamber closure times. During NEE measurements PAR values were logged every 5 s, and subsequently corrected for the effect of the acrylic glass PAR reduction. Measurements were stopped when the temperature difference between inside the chamber and ambient air temperature exceeded 1.5 °C, and repeated if the minimum closure time was not reached (cf. Leiber-Sauheitl et al. 2014). In total we conducted 19 (Carex grassland, 1-cut) or 20 (intensive grassland, 2-cuts) measurement campaigns with a minimum of 5 NEE and 5 R_{eco} measurements per plot during 7 h in winter, and a maximum of 12 NEE and 8 R_{eco} measurements per plot during 11 h in summer. Extensions were used when the vegetation height exceeded 50 cm (maximum of 1 m height and 612 L chamber volume). In case of snow cover, the snow on the collars was carefully removed to guarantee gas tightness of the chambers.

CO₂ flux calculations were done in R (R Core Team 2022) using a modified version of the package *flux* (version 0.3-0, Jurasinski et al. 2014; modification Schlaipfer et al. in prep.): the optimization algorithm was modified to select the model with the steepest slope rather than choosing the model with the highest R² as long as all necessary assumptions of linear regression were fulfilled ($\alpha=0.05$). NEE flux calculations further included a minimum of 7 data points (=30 s), R² as the statistic used to find the linear part, and the IRGA detection limit of 1.5 ppm. For R_{eco} flux calculations we included a minimum of 13 data points (=60 s).

Modelling of R_{eco} and gross primary production (GPP) was done in R. For each measurement campaign and treatment, the dependency between R_{eco} and temperature (T_{air}, ST2, ST5 or ST10) was modelled according to Lloyd and Taylor (1994: Eq. 11).

$$R_{eco} = R_{ref} \times e^{E_0} \times ((1/T_{ref} - T_0) - 1/T - T_0), \quad (1)$$

where R_{eco} is the ecosystem respiration [mg CO₂-C m⁻² h⁻¹], R_{ref} is the respiration at the reference temperature [mg CO₂-C m⁻² h⁻¹], E₀ is the activation energy [K], T_{ref} is the reference temperature 283.15 [K], T₀ is the temperature constant for the start of biological processes: 227.13 [K], and T is air or soil temperature [K].

The R_{eco} model was fitted to the temperature (T_{air}, ST2, ST5 or ST10) which showed the best explanatory power for R_{eco}. Consecutive campaigns were pooled when no statistically significant relationship between a temperature and R_{eco} fluxes in one campaign could be found. An average CO₂ flux was calculated for measurement campaigns during snow cover or if campaign pooling did not result in a statistically significant relationship between temperature and the pooled R_{eco} fluxes. Half-hourly R_{eco} fluxes were calculated from the model parameters R_{ref} and E₀, and the time series of measured air and soil temperatures. Fluxes between two consecutive campaigns were calculated by using the parameters of the first campaign to model forwards, and from the second campaign to model backwards. Subsequently, 0.5-h values were calculated from the distance weighted average of both fluxes. In case of harvesting and during snow cover we kept model parameters constant up to the event. After harvest or end of snow cover parameters from the subsequent measurement campaign were used (Leiber-Sauheitl et al. 2014). The total annual R_{eco} was the sum of the modelled 0.5-h R_{eco} fluxes.

GPP values were calculated by subtracting the temporally corresponding modelled R_{eco} flux from the measured NEE flux. GPP was then modelled based on calculated campaign fluxes with PAR as the explanatory variable adapted from the Michaelis–Menten type rectangular hyperbolic function proposed by Falge et al. (2001, equation A.9).

$$GPP = \alpha \times PAR / (1 - (PAR/2000) + (\alpha \times PAR/GPP2000)), \quad (2)$$

where GPP is gross primary production [mg CO₂-C m⁻² h⁻¹], α is the initial slope of the curve or light use efficiency [mg CO₂-C m⁻² h⁻¹/μmol quantum m⁻² s⁻¹], PAR is the photon flux density of the photosynthetically active radiation [μmol quantum m⁻² s⁻¹], and GPP2000 is the gross primary

production at PAR $2000 \mu\text{mol quantum m}^{-2} \text{s}^{-1}$ [$\text{mg CO}_2\text{-C m}^{-2} \text{h}^{-1}$].

Half-hourly GPP fluxes were calculated using the same approach as for R_{eco} . Snow cover was treated as described above. In the case of harvest, α and GPP2000 were kept constant from the preceding measurement until the management time and were set to zero at the 0.5-h time step during the working process. Thereafter, parameters were linearly interpolated from the subsequent measurement campaign for the grassland plots (cf. Eickenscheidt et al. 2015). The total annual GPP was the sum of the modelled 0.5-h GPP fluxes.

In this study we follow the atmospheric sign convention where R_{eco} is positive and GPP negative, and NEE and total GHG balances are positive for a net source (a release from ecosystem to the atmosphere) and negative for a net sink (a sequestration from the atmosphere into the ecosystem).

To account for the uncertainties in annual R_{eco} and annual GPP modelling, annual sums from the upper and lower limits of the determined parameters (R_{ref} , E_0 , α , GPP2000), based on their standard errors (SE) were estimated and are recorded as range (Drösler 2005; Elsgaard et al. 2012; Eickenscheidt et al. 2015). An overview of all model parameters is given in Supplementary Tables S2–5.

CH₄ and N₂O gas flux measurements and flux calculation

We determined CH₄ and N₂O fluxes weekly from December 2016 to January 2018 between 09:00 and 11:00 am ('daily mean temperature' time) using the static manual chamber method (Livingston and Hutchinson 1995) with opaque chambers. At each gas flux measurement event, four gas samples were drawn from the chamber headspace in 20-min intervals over the chamber closure period of 60 min. Each gas sample was collected in a 20 mL glass vial sealed with a butyl rubber septum. Before sample collection, the vials were flushed with chamber air for 30 s (32 times vial air exchange). Sample air was pressurized using a micro pump (NMP015B, KNF Neuberger) to approximately 0.5 bar to prevent inflow of ambient air into the vials prior to lab analysis. Concentrations of CH₄ and N₂O were determined using a gas chromatograph (Clarus 480 GC, PerkinElmer Inc.) equipped with a headspace autosampler (TurboMatrix 110,

PerkinElmer Inc.), Porapak 80/100 mesh column for gas species separation, methanizer interfaced with a flame ionization detector (FID, temperature 350 °C) for CH₄ and CO₂, and an electron capture detector (ECD, temperature 380 °C) for N₂O determination.

Gas fluxes were calculated by fitting linear or non-linear (diffusion-based) concentration–time (flux) models to the measured data using the R package *gasfluxes* with standard settings (version 0.4, Fuß et al. 2020) and considering atmospheric pressure and chamber air temperature at the time of gas flux measurements. We selected between the linear model fit and the exponential model fit (HMR model using the Golub-Pereyra algorithm for partially linear least-squares) using the recommended selection function provided in the *gasfluxes* package (selection algorithm restricts nonlinearity by imposing a maximum value for kappa). For CH₄, we only allowed nonlinear calculation when fluxes were within 20% of the calculated robust linear flux (arbitrary value) to reduce the uncertainty of overestimation of the four-point data set (nonlinear fluxes 69 of 1198 fluxes = 5.8%). N₂O flux values $< -50 \mu\text{g m}^{-2} \text{h}^{-1}$ were excluded from the calculation as strong negative N₂O fluxes are impossible due to the laws of physics and as recommended by Fuß (personal communication 2015) (excluded 33 of 1198 fluxes = 2.8%). We calculated annual plot-specific gas balances by linear interpolation of the measured plot fluxes. Annual gas balances were then averaged over the three replicates to give treatment-specific annual gas balances and are reported with standard error (SE).

Carbon balance and total greenhouse gas emissions

We determined the carbon balance of each treatment under consideration of C gas fluxes from CO₂ and CH₄, and C_{org} import via fertilization (intensive grassland only) and C_{org} export via harvest (Elsgaard et al. 2012). Net C balance was therefore:

$$\begin{aligned} \text{Net C balance (t C ha}^{-1} \text{ year}^{-1}) \\ = \text{NEE (t CO}_2\text{-C ha}^{-1} \text{ year}^{-1}) \\ + \text{C}_{\text{org}} \text{ import and export (t C ha}^{-1} \text{ year}^{-1}) \\ + \text{CH}_4 \text{ (t CH}_4\text{-C ha}^{-1} \text{ year}^{-1}) \end{aligned} \quad (3)$$

The net climate effect of a treatment can be deduced from the summed CO₂-equivalent (CO₂-eq) emissions of the observed GHG fluxes, and C imports and exports. We used the 100-year time horizon global warming potentials (GWP100) of 28 for CH₄ and 265 for N₂O given in IPCC Assessment Report IPCC AR5 (Myhre et al. 2013) as used in the German national GHG inventory reporting. To include biomass C exports and fertilizer C imports in the CO₂-eq balance of a treatment, we converted t C ha⁻¹ year⁻¹ to t CO₂ ha⁻¹ year⁻¹ by multiplying by the ratio of the molecular weight of carbon dioxide (44.01 g mol⁻¹) to that of carbon (12.01 g mol⁻¹):

$$\text{t CO}_2 \text{ ha}^{-1} \text{ year}^{-1} = \text{t biomass or fertilizer C}_{\text{org}} \times (44.010 \text{ units CO}_2 / 12.011 \text{ units C}) \quad (4)$$

Statistical analysis

We used R for statistical data analyses (R Core Team 2022). Differences in annual biomass yield and annual CO₂ emissions of treatments were determined using a multifactorial analysis of variance (ANOVA). We used diagnostic plots to assess fulfillment of criteria in the respective final model (see Crawley 2007). The Shapiro–Wilk normality test was conducted to evaluate normal distribution of residuals and the studentized Breusch–Pagan test to evaluate homogeneous variances. In the plot-specific yield data, we additionally used Tukey’s honestly significant difference test as the post-hoc test.

Due to temporal pseudoreplication of the time series data (GWL, temperature, all GHGs), we used linear mixed effects (lme) models (Crawley 2007; Hahn-Schöfl et al. 2011; Eickenscheidt et al. 2015). We followed the approach suggested by Zuur et al. (2009) to set up the lme models in a top-down strategy using the *nlme* package (Pinheiro et al. 2023). First, the random structure with a full model in the fixed term was optimized, followed by an optimization of the fixed structure. Successively, non-significant terms were removed from the fixed model structure. Model requirements were assessed by plotting quantile–quantile plots and histograms of residuals. Homoscedasticity was evaluated by plotting the residuals against the fitted values. Validity of all model

simplifications and extensions (autocorr functions, variance functions) was evaluated with AIC. We use the general linear hypothesis function from the *multcomp* package (Hothorn et al. 2021) to conduct Tukey contrasts for multiple comparison. To compare specified factors or factor combinations in our lme models we used the estimated marginal means function from the package *emmeans* (Lenth et al. 2021). We accepted significant differences if $p \leq 0.05$. Results in the text are given as mean \pm 1 standard deviation.

To test for the success of warming on soil temperature in -0.02 m depth (ST2), we set up a lme model containing the mean annual ST2 as the target vari-

able, temperature factor (‘ambient’ or ‘warming’) and grassland type (‘intensive’ or ‘Carex’) as the explanatory variables (fixed effects), and with ‘plot’ as the random factor. The overall success of rewetting was assessed using the mean annual GWL as the target variable, the GWL factor (‘drained’ or ‘rewetted’) as the explanatory variable, and with ‘treatment’ as the random factor. To analyze differences in the mean annual GWL between the individual treatments, the final lme model contained treatment as the explanatory variable, and ‘plot’ as the random factor. Significant differences in the annual N₂O emissions were assessed with the final lme model containing GWL_factor + grassland_type \times temp_factor as the explanatory variable and ‘plot’ as the random factor. The lme model for annual CH₄ emissions had GWL_factor \times grassland_type as the explanatory variable and ‘plot’ as the random factor. Due to observed heteroscedasticity, we extended the CH₄ and N₂O models by a variance function. Lme models to compare means of modelled daily R_{eco} and GPP fluxes had the same structure with the explanatory variables GWL_factor \times temperature_factor + grassland_type and the random factors of ‘plot’ nested within ‘campaign’. We observed autocorrelation and heteroscedasticity in both lme models. Hence, we included an autocorrelation function and a variance function.

Results

Environmental drivers

The weather conditions of the study year were similar to the long-term average (1993–2022) for the region. In 2017, monthly mean air temperature at 2 m height ranged from -5.5°C in January to 19.0°C in July with an annual mean of 9.2°C , and a total precipitation of 751.4 mm as recorded by the climate station of the German weather service at the Munich airport (DWD 2023). The on-site annual mean air temperatures at 0.2 m height were 9.1°C (daily mean range -14.8°C in January to 25.1°C in July) and at 2 m height 9.2°C (daily mean range -13.8°C in January to 24.8°C in August).

Passive warming resulted in an average increase of annual mean air temperature in 0.2 m height of $+0.93^{\circ}\text{C}$ (0.79 to 1.26°C) across all warming treatments with slightly less warming in the rewetted intensive grassland and both Carex grassland treatments (Table 2, see Supplementary Figure S1 for details on the OTC effects). The OTC effect varied during the year, with higher impact on air temperatures during the coldest periods observed in January, and in the beginning of the vegetation period where ambient temperatures increased, and plant height was still low. Daily mean air

temperature at the research site in 0.2 m was below 0°C on 46 days. Passive warming decreased the number of days below 0°C to 42 days. A snow cover from 4 to 31 January 2017 was followed by seven weeks of freeze–thaw cycles in all treatments. During the freeze–thaw period, warming by OTCs had a minor effect increasing T_{air} by 0.2°C on average. Warming significantly ($p < 0.0001$) increased the overall mean annual soil temperature by $+0.6^{\circ}\text{C}$ in -0.02 m depth (ST2) across all warming treatments (mean of IDW, IRW, CDW and CRW) compared to all ambient treatments (mean of IDA, IRA, CDA and CRA). Independent of warming, significantly ($p < 0.0001$) higher mean annual ST2 were found in the intensive grassland compared to the Carex grassland (Table 2). Groundwater level had no significant effect on warming.

The mean annual groundwater levels were between -0.30 to -0.39 m (range -0.75 m to 0.06 m) in the drained treatments and between -0.13 to -0.14 m (range -0.44 m to 0.04 m) in the rewetted treatments during the manipulation period (Table 2; Fig. 2). The annual mean groundwater levels were significantly ($p < 0.0001$) increased as intended at the rewetted treatments compared to the drained treatments in both grassland systems. In the drained basin, the GWL of the intensive grassland was significantly ($p < 0.0001$) higher than the GWL

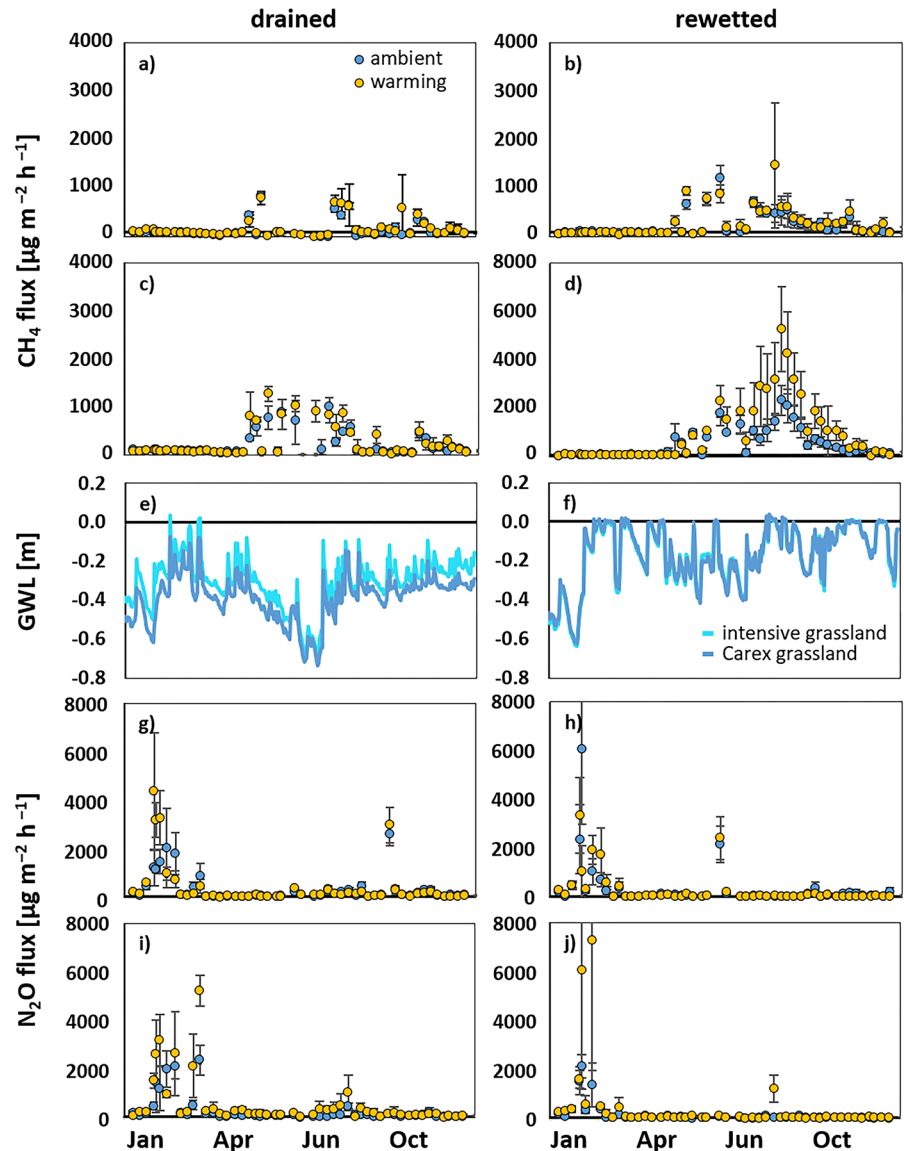
Table 2 Summary of the annual mean, the minimum and maximum air and soil temperatures and the groundwater levels in the eight treatments for 2017

Treatment	Tair (min/max)	Tsoil (min/max)			GWL (min/max)	
	0.2 m	−0.02 m	−0.05 m	−0.1 m	Relative to soil surface	
	°C	°C	°C	°C	m	
					Full year 01.01.–31.12.2017	GWL manipulation 07.02.–31.12.2017 ^a
IDA	9.2 (−22.6/34.9)	10.5 (−1.9/30.7)	10.8 (−0.7/29.6)	10.7 (−0.1/24.7)	− 0.32 (−0.71; 0.05)	
IDW	10.1 (−20.8/39.6)	11.2 (−2.6/32.5)	11.4 (−0.4/28.7)	11.4 (1.2/25.2)	− 0.30 (−0.71; 0.06)	
IRA	9.1 (−22.7/37.6)	10.6 (−1.9/29.4)	10.4 (−1.7/27.2)	10.5 (0.1/24.1)	− 0.17 (−0.65; 0.03)	− 0.13 (−0.40; 0.03)
IRW	10.3 (−21.1/38.0)	10.8 (−2.6/32.7)	10.7 (−1.2/29.2)	10.7 (0.5/27.6)	− 0.17 (−0.68; 0.02)	− 0.14 (−0.40; 0.02)
CDA	9.1 (−22.2/33.8)	9.3 (−2.6/22.9)	10.8 (−0.1/21.1)	11.1 (−0.1/20.7)	− 0.39 (−0.75; −0.05)	
CDW	9.9 (−19.4/34.0)	9.9 (−3.2/23.8)	11.5 (−0.6/21.4)	11.6 (−0.1/21.0)	− 0.39 (−0.75; −0.06)	
CRA	9.0 (−22.7/34.9)	9.4 (−2.9/22.2)	9.6 (−2.5/21.7)	9.6 (−0.6/20.8)	− 0.16 (−0.63; 0.04)	− 0.13 (−0.43; 0.04)
CRW	9.8 (−19.3/38.2)	10.3 (−3.2/25.8)	10.2 (−2.5/23.7)	10.2 (−1.1/21.0)	− 0.17 (−0.67; 0.04)	− 0.13 (−0.44; 0.04)

I intensive grassland, C Carex dominated grassland, D drained, R rewetted, A ambient temperature, W warming via OTCs

^aGWL manipulation started on 06.02.2017

Fig. 2 Time series of measured mean CH_4 campaign fluxes [$\mu\text{g CH}_4 \text{ m}^{-2} \text{ h}^{-1}$] **a** IDA and IDW, **b** IRA and IRW, **c** CDA and CDW, **d** CRA and CRW, mean water levels [GWL in m] of the intensive and Carex grassland for the drained grasslands for the drained treatments (**e**) and rewetted treatments (**f**), and measured mean N_2O campaign fluxes [$\mu\text{g N}_2\text{O m}^{-2} \text{ h}^{-1}$] **g** IDA and IDW, **h** IRA and IRW, **i** CDA and CDW, **j** CRA and CRW) in 2017. GWL manipulation started on 06-02-2017. Note that the y-axis of mean CH_4 campaign fluxes in (**d**) has a two times greater magnitude



of the Carex treatments due to the slight slope in the surface terrain. Warming had no significant effect on GWL. Groundwater levels in all treatments showed dynamic fluctuations throughout the year with low levels in summer and high levels in winter, and with similar responses to heavy rainfall events e.g. in July and August (see Fig. 2).

Aboveground plant productivity

Overall, biomass productivity in the Carex treatments with up to $14.3 \pm 1.0 \text{ t DM ha}^{-1} \text{ year}^{-1}$ (CRA) was significantly ($p < 0.0001$) higher compared with the intensive treatments with maximum biomass development of $9.6 \pm 1.2 \text{ t DM ha}^{-1} \text{ year}^{-1}$ (IDW). Warming resulted in an increase of 30% in biomass yield of the ID treatments while the effect was negative with up to -12% in all other

Table 3 Annual ecosystem respiration (R_{eco}), gross primary production (GPP), and net ecosystem exchange (NEE) rates (given with range), as well as C import through organic fertilizer and C export from biomass harvest, annual exchange rates of methane (CH_4) and nitrous oxide (N_2O) (means \pm standard errors), resulting net carbon balance and total GHG balances according to IPCC AR5 metrics (as used in NIR as of 2023)

Treatment	R_{eco}	GPP	NEE	C export	C import	CH_4	N_2O	C balance	GHG balance
	$t\ CO_2\ ha^{-1}\ year^{-1}$	$t\ CO_2\ ha^{-1}\ year^{-1}$	$t\ CO_2\ ha^{-1}\ year^{-1}$	$t\ C\ ha^{-1}\ year^{-1}$	$t\ C\ ha^{-1}\ year^{-1}$	$kg\ CH_4\ ha^{-1}\ year^{-1}$	$kg\ N_2O\ ha^{-1}\ year^{-1}$	$t\ C\ ha^{-1}\ year^{-1}$	$t\ CO_2\ eq\ ha^{-1}\ year^{-1}$
IDA	133.4 (118.6/153.7)	-99.1 (-105.4/-92.5)	34.3 (13.2/61.2)	3.3 \pm 0.3	1.2 \pm 0.0	1.9 \pm 0.3	24.6 \pm 2.6	11.4 (5.4/19.0)	48.4 (25.6/77.0)
IDW	154.9 (135.7/177.9)	-106.7 (-116.8/-95.7)	48.2 (19.0/82.2)	4.3 \pm 0.3	1.2 \pm 0.0	5.4 \pm 1.3	27.4 \pm 5.7	16.2 (7.9/25.8)	66.9 (34.9/103.5)
IRA	104.9 (94.1/117.3)	-96.0 (-100.7/-91.0)	8.9 (-6.6/26.3)	2.9 \pm 0.1	1.2 \pm 0.0	13.5 \pm 1.1	20.8 \pm 0.6	4.1 (-0.3/8.9)	20.6 (4.6/38.8)
IRW	98.4 (86.3/112.5)	-89.7 (-95.7/-83.2)	8.7 (-9.5/29.3)	2.8 \pm 0.2	1.2 \pm 0.0	16.4 \pm 2.3	22.6 \pm 0.7	4.0 (-1.2/9.8)	21.0 (1.6/42.6)
CDA	121.7 (112.6/131.4)	-134.1 (-144.1/122.8)	-12.4 (-31.5/8.5)	6.4 \pm 0.2	-	9.2 \pm 1.9	20.0 \pm 2.9	3.1 (-2.3/9.0)	16.8 (-3.7/39.1)
CDW	136.0 (118.5/156.1)	-146.3 (-157.3/-134.4)	-10.3 (-38.7/21.6)	6.2 \pm 0.4	-	14.4 \pm 1.6	39.7 \pm 2.7	3.5 (-4.7/12.5)	23.5 (-7.2/57.5)
CRA	110.3 (92.7/131.1)	-148.2 (-158.6/-136.7)	-38.0 (-65.9/-5.6)	6.4 \pm 0.2	-	39.2 \pm 6.3	8.8 \pm 1.3	-3.9 (-11.8/5.2)	-11.1 (-40.5/22.8)
CRW	84.8 (72.4/102.9)	-128.1 (-137.1/-118.3)	-43.3 (-64.7/-15.4)	5.7 \pm 0.4	-	76.5 \pm 21.8	27.0 \pm 7.0	-6.1 (-12.4/2.0)	-13.1 (-38.5/18.8)

treatments. Rewetting of the intensive treatments reduced yields by 10% under ambient and by 31% under warming conditions, however, the effect was barely not significant ($p=0.0527$). Rewetting had no significant effect on biomass yield in the *Carex* treatments.

CH_4 exchange

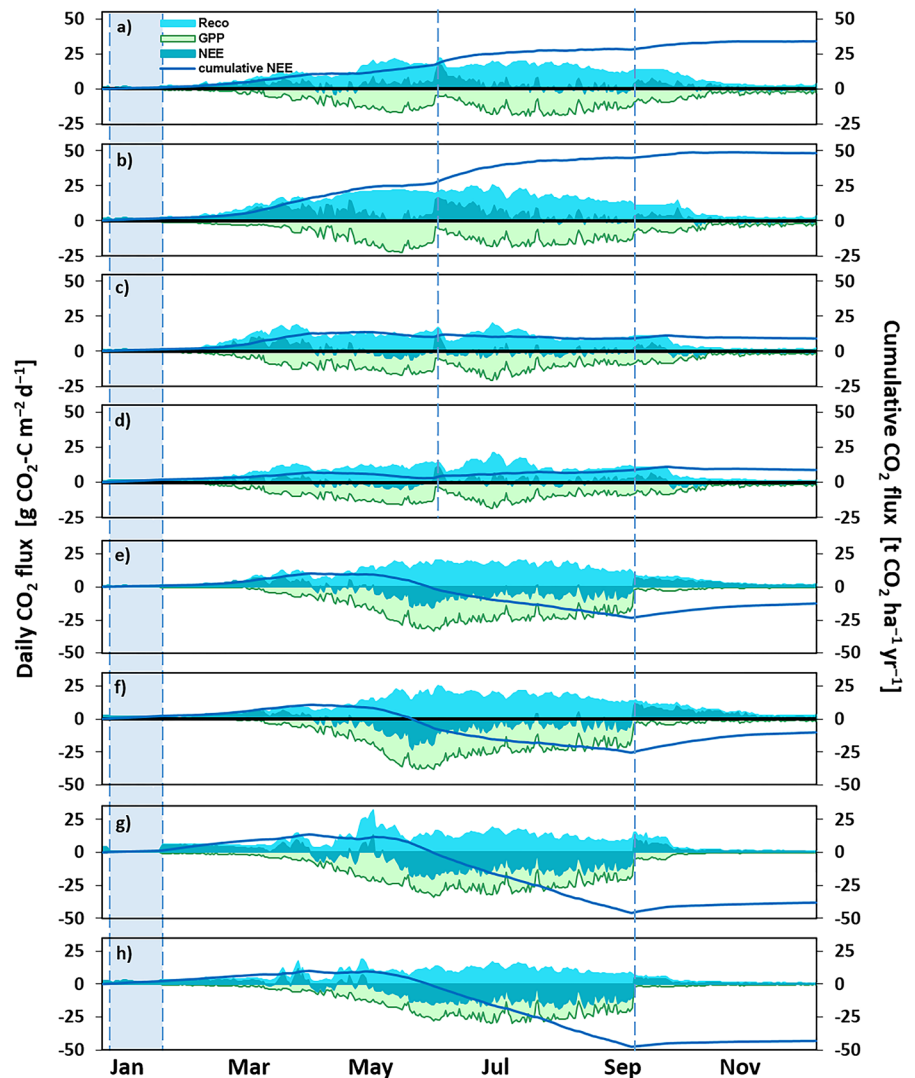
The CH_4 fluxes showed a clear seasonal pattern on both land use types with peak emissions in the summer when groundwater levels and/or soil temperatures were high (Fig. 2). In the intensive grassland, maximum measured hourly fluxes ranged from $718 \pm 141\ \mu g\ CH_4\ m^{-2}\ h^{-1}$ in IDW to $1409 \pm 1328\ \mu g\ CH_4\ m^{-2}\ h^{-1}$ in IRW. In the *Carex* grassland, maximum hourly CH_4 fluxes were higher compared to the intensive grassland ranging from $929 \pm 199\ \mu g\ CH_4\ m^{-2}\ h^{-1}$ in CDA to $5246 \pm 1772\ \mu g\ CH_4\ m^{-2}\ h^{-1}$ in CRW. During winter and spring (mid December–mid May), CH_4 fluxes were $< 100\ \mu g\ CH_4\ m^{-2}\ h^{-1}$ or slightly negative (max uptake $-157 \pm 116\ \mu g\ CH_4\ m^{-2}\ h^{-1}$ in IRA in December 2016) in all treatments.

Significantly ($p < 0.0001$) higher annual CH_4 emissions were observed in the *Carex* grassland compared to the intensive grassland (see Table 3 for annual mean values \pm SE). We observed the highest annual CH_4 exchange rates in the rewetted *Carex* amounting to $39 \pm 6\ kg\ CH_4\ ha^{-1}\ year^{-1}$ under ambient (CRA) and $77 \pm 22\ kg\ CH_4\ ha^{-1}\ year^{-1}$ under warming conditions (CRW). Moreover, the lowest emissions were found in the drained intensive grassland with $2 \pm 0\ kg\ CH_4\ ha^{-1}\ year^{-1}$ in IDA and $5 \pm 1\ kg\ CH_4\ ha^{-1}\ year^{-1}$ in IDW. Overall, rewetting significantly ($p < 0.0001$) enhanced the annual CH_4 exchange in all treatments. While temperature increase resulted in higher annual CH_4 budgets in all treatments compared to the respective ambient air temperature treatment, the warming effect was not statistically significant.

N_2O exchange

During the 2017 measurement period, N_2O fluxes showed one distinct peak period in early February following snowmelt and water level increase, and lasting for seven weeks (Fig. 2g–j). During this period, maximum measured fluxes in the intensive grassland ranged from $2005 \pm 1646\ \mu g\ N_2O\ m^{-2}\ h^{-1}$ in IDA to $6066 \pm 3122\ \mu g\ N_2O\ m^{-2}\ h^{-1}$ in IRA. In

Fig. 3 Time series of modeled daily CO_2 fluxes [$\text{g CO}_2\text{-C m}^{-2} \text{d}^{-1}$] and cumulative NEE [$\text{t CO}_2 \text{ha}^{-1} \text{year}^{-1}$] for each treatment in 2017: **a** IDA, **b** IDW, **c** IRA, **d** IRW, **e** CDA, **f** CDW, **g** CRA, **h** CRW. Grey bar marks the period with snow cover 04 to 31 Jan 2017. Dashed lines indicate management activities: two harvest and fertilizing events in the intensive grassland (**a–d**), one harvest event in the Carex dominated grassland (**e–h**). Note that the y-axes for the two grassland types differ in magnitude



the Carex grassland, maximum N_2O fluxes were higher compared to the intensive grassland ranging from $2108 \pm 470 \mu\text{g N}_2\text{O m}^{-2} \text{h}^{-1}$ in CRA to $7261 \pm 5322 \mu\text{g N}_2\text{O m}^{-2} \text{h}^{-1}$ in CRW. N_2O peak emissions amounted to 43 to 48% of total annual N_2O emissions in the intensive treatments and between 55 to 79% in the Carex treatments. Fertilization resulted in a distinct increase of N_2O fluxes in the week following application only in June in the rewetted treatments, whereas the drained treatments showed this behavior only after September application. In most cases, annual N_2O emissions were significantly ($p < 0.0001$) higher under drained conditions, and under warming conditions ($p < 0.0001$) (see Table 3 for annual mean values \pm SE). We

observed the highest annual N_2O emissions in CDW with $40 \pm 3 \text{ kg N}_2\text{O ha}^{-1} \text{year}^{-1}$, and the lowest in CRA with $9 \pm 1 \text{ kg N}_2\text{O ha}^{-1} \text{year}^{-1}$.

CO_2 exchange

CO_2 exchange dynamics followed general seasonal and management-related trends responding to air and soil temperatures, PAR, and harvest events (Fig. 3). However, the responses to the environmental drivers differed in magnitude between the plant communities and water levels. The measured R_{eco} fluxes in the intensive grassland were significantly ($p < 0.0001$) higher compared with the Carex grassland. Drained conditions in both grassland types led to significantly

($p < 0.0001$) higher R_{eco} fluxes. Warming resulted in significantly ($p < 0.0001$) higher R_{eco} fluxes under drained conditions, while the opposite was observed under rewetted conditions. On the treatment level, R_{eco} reached daily maxima of up to $25.7 \text{ g CO}_2\text{-C m}^{-2} \text{ d}^{-1}$ in the intensive grassland (IDW in July) and up to $32.2 \text{ g CO}_2\text{-C m}^{-2} \text{ d}^{-1}$ in the Carex grassland (CRA in May). Overall, the R_{eco} flux models in our study were driven by Tair (62% of 140 R_{eco} models) and ST2 (19%). Soil temperatures ST5 and ST10 were each used in less than 5% of the models whereas no model could be fitted in 11% of the campaigns.

Calculated GPP fluxes were significantly ($p < 0.0001$) higher in the Carex grassland. While individually neither temperature nor water level had significant effects on GPP fluxes, there was a significant ($p < 0.0001$) increase of GPP under drained and warming conditions. Maximum daily GPP uptakes were $-22.6 \text{ g CO}_2\text{-C m}^{-2} \text{ d}^{-1}$ in the intensive grassland (IDW in June) and $-37.8 \text{ g CO}_2\text{-C m}^{-2} \text{ d}^{-1}$ in the Carex grassland (CDW in June). In 91% of all campaigns, GPP models were fitted with PAR. Model parameters for all R_{eco} and GPP models are listed in the Supplementary Tables S2–5.

Regarding annual R_{eco} emissions, rewetting resulted in a significant ($p = 0.00573$) reduction. In general, neither grassland type nor warming had a significant effect on annual R_{eco} emissions. Annual GPP uptake was significantly ($p < 0.0005$) higher in the Carex grassland compared with the intensive grassland. In general, neither rewetting nor warming had a significant effect on annual GPP uptake. Annual NEE emissions were significantly ($p < 0.0001$) reduced by the shift in grassland management. We observed that all intensive grassland treatments remained cumulative sources of NEE CO_2 throughout the year (R_{eco} outweighs GPP), while all Carex grassland treatments turned into NEE CO_2 sinks in June (cumulative NEE turns negative). Rewetting significantly ($p < 0.0005$) reduced the annual NEE emissions whereas warming had no significant effect. Largest annual NEE CO_2 exchange was found in IDW with 48.2 (range 19.0 to 82.2) $\text{t CO}_2 \text{ ha}^{-1} \text{ year}^{-1}$, while CRW showed the largest NEE CO_2 uptake of -43.3 (range -64.7 to -15.4) $\text{t CO}_2 \text{ ha}^{-1} \text{ year}^{-1}$ (see Table 3).

Carbon balance and total greenhouse gas emissions

Under rewetted conditions both Carex grassland treatments were C sinks amounting to -3.9 (CRA; range 5.2 to -11.8) under ambient and -6.1 (CRW; range 2.0 to -12.4) $\text{t C ha}^{-1} \text{ year}^{-1}$ under warmed conditions. All other treatments were C sources, which in the drained Carex treatments was attributable to large harvest C exports. Intensive grassland under drained conditions exhibited the largest C source (see Table 3).

The total GHG balances of the studied grassland systems further include N_2O emissions (see Table 3 for annual GHG balance means and ranges). Again, both Carex grassland treatments under rewetted conditions functioned as strong net GHG sinks with annual GHG balances of -11.1 (CRA; range -40.5 to 22.8) and -13.1 (CRW; range -38.5 to 18.8) $\text{t CO}_2\text{-eq ha}^{-1} \text{ year}^{-1}$. Likewise, intensive grassland under drained conditions remained the largest net GHG sources with annual GHG balances of 48.4 (IDA; range 25.6 to 77.0) and 66.9 (IDW; range 34.9 to 103.5) $\text{t CO}_2\text{-eq ha}^{-1} \text{ year}^{-1}$. The relative contribution of net C fluxes in the GHG budgets were between 77 (IRW) and 89% (IDW) in the intensive grassland treatments and between 73 (CDW) and 95% (CRA) in the Carex grassland treatments.

Discussion

Status quo of drained intensive grassland on organic soils

Under ambient conditions, the drained intensive grassland (IDA) was representative of the current land use conditions in the surrounding area. The GWL of the drained intensive grassland in this study of -0.32 m relative to the surface is slightly higher but within the standard deviation of the German average GWL for grassland on organic soil of $-0.44 \pm 0.29 \text{ m}$ (Bechhold et al. 2014) and could thus be considered as ‘moderately drained’. The net annual GHG emissions of the drained intensive grassland of $48.4 \text{ t CO}_2\text{-eq ha}^{-1} \text{ year}^{-1}$ in this study exceed the IPCC emission factors (EFs) for grassland on drained organic soils ranging from 14 to $27 \text{ t CO}_2\text{-eq ha}^{-1} \text{ year}^{-1}$ (Tier 1 approach: range of nutrient-poor,

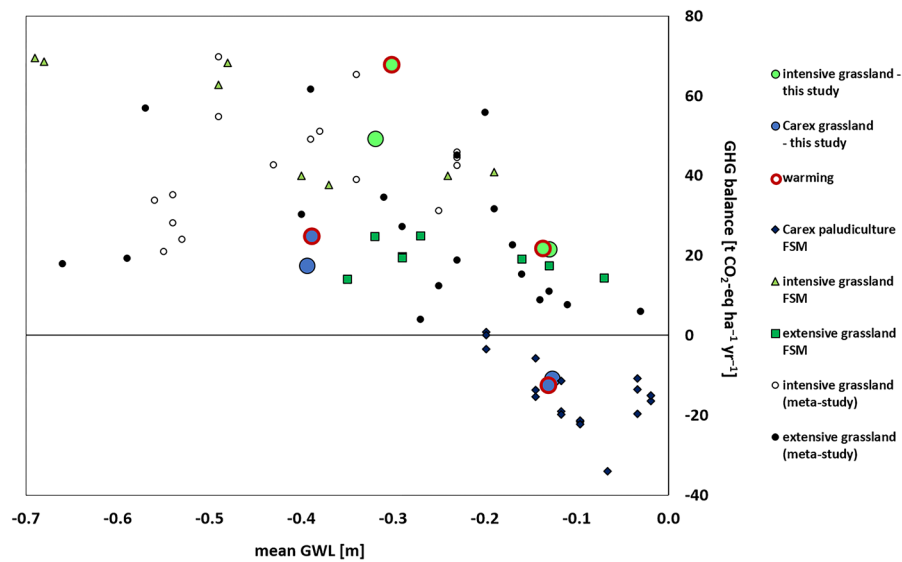


Fig. 4 Relationship between mean annual ground water levels (GWL in m below the surface) and total greenhouse gas emissions (GHG balance in $\text{t CO}_2\text{-eq ha}^{-1} \text{ year}^{-1}$) for the eight intensive and Carex dominated grassland treatments of this study. For comparison, GHG emissions are presented for intensive grassland (2–3 cuts, $113\text{--}220 \text{ kg N ha}^{-1} \text{ year}^{-1}$ fertilization) and extensive grassland (1 cut, no fertilization) from previous studies in the Freisinger Moos (FSM; Drösler et al. 2013;

Eickenscheidt et al. 2014, 2015; Metzger et al. 2015; Tiemeyer et al. 2016 as given in Tiemeyer et al. 2020), and GHG emission values for newly established (planted) Carex paludicultures from an adjacent research site measured 2019–2021 (Bockermann et al. in prep, MOORuse project results). Further GHG balances for intensive and extensive grassland on organic soils from various sites in Germany are included as reported in Tiemeyer et al. (2020)

shallow-drained, nutrient-rich and deep-drained, nutrient rich-grasslands; IPCC 2014). Our emissions are also at the higher end of the current German EF of 31.7 (5 to 52) $\text{t CO}_2\text{-eq ha}^{-1} \text{ year}^{-1}$ for grassland on drained organic soils (Tier 2 approach) given by Tiemeyer et al. (2020). However, previous studies in this region have documented comparably elevated values. Eickenscheidt et al. (2015) reported net GHG emissions of $59 (\pm 33) \text{ t CO}_2\text{-eq ha}^{-1} \text{ year}^{-1}$ for a grassland site under comparable management with three harvests, fertilization with $155 \text{ kg N}_{\text{tot}} \text{ ha}^{-1} \text{ year}^{-1}$ cattle slurry, and at a mean annual GWL of -0.52 m , but lower C_{org} content in the upper 20 cm top soil layer. Poyda et al. (2016) found comparably high emissions of $65.3 \text{ t CO}_2\text{-eq ha}^{-1} \text{ year}^{-1}$ in a moderately drained grassland (GWL of -0.33 m) but with greater management intensity ($260 \text{ kg N}_{\text{tot}} \text{ ha}^{-1} \text{ year}^{-1}$ slurry input). Our findings are consistent with the total GHG emissions from intensive grassland reported in Tiemeyer et al. (2020) as shown in Fig. 4.

Mitigation measures

Plant community shift and management extensification

Mitigation via a plant community shift toward *Carex acutiformis* combined with a management extensification successfully reduced the large net emissions observed in the intensively managed drained grassland by 65% (IDA vs. CDA). One main aspect leading to the disproportionally large GHG emissions in intensive grassland systems is N fertilization, which enhances soil organic matter decomposition and consequently heterotrophic respiration (R_h ; Kasimir-Klemetsson et al. 1997). The adjusted N fertilization in intensive agricultural practice further leads to an increase in the cutting frequency to optimize biomass yields and forage quality. This promotes the dominance of certain grassland species. The species composition in particular has an important influence on R_{eco} , GPP, NEE and finally on the total GHG balance. This is also clearly reflected in our study where the Carex dominated

grassland with a late-season harvest (CDA) resulted in distinctly greater biomass development, evident through increased GPP and nearly double the biomass yield compared with the intensive grassland. The isolated effect of transplanting soil-monoliths with adult plants on biomass growth in the following years was not found in literature. Thus, it cannot be completely ruled out that the transplanting of *Carex* led to an increased biomass growth, particularly of roots and rhizomes, in the study year. Compared with the intensive grassland, all *Carex* treatments exhibited decreased net CO₂ emissions, while we observed higher CH₄ emissions. The latter is an anticipated outcome of transitioning to wetland-adapted plants like *Carex*, where physiological and biochemical adaptations interact (e.g., Baird et al. 2009; Waldo et al. 2019). First, *Carex* roots can grow into the anaerobic soil layer supplying readily available C sources for methanogenesis through root exudates (Whalen 2005; Ward et al. 2013). Second, aerenchymatous tissue in the plant stems enable direct diffusion of greater amounts of CH₄ produced in the soil into the atmosphere. Due to the extensive peak emissions in February and March, the shift to extensive management without fertilizer application did not result in significantly lower N₂O emissions (IDA 24.6 vs. CDA 20.8 kg N₂O ha⁻¹ year⁻¹). This contrasts with a European meta-study by Leppelt et al. (2014) who found that grassland N₂O fluxes of drained organic soils are intricately linked to the amount of applied N. In general, observed N₂O emissions in all treatments are notably higher compared to the implied national emission factor for grassland of 4.2 kg N₂O-N ha⁻¹ year⁻¹ (Tiemeyer et al. 2020), but within the range of reported N₂O emissions from drained organic grassland sites in literature of 1 to 145 kg N₂O-N ha⁻¹ year⁻¹ (Velthof et al. 1996; Flessa et al. 1998; van Beek et al. 2010, 2011; Petersen et al. 2012; Eickenscheidt et al. 2014; Offermanns et al. 2023). In the present study, 43 to 79% of the annual N₂O emissions were related to a pronounced peak emission period where freeze–thaw cycles after snow-cover and a distinct increase in water level coincided (Fig. 2). It is well known that freeze–thaw conditions promote pulses of N₂O emissions, which can significantly dominate the annual budgets (Flessa et al. 1998; Butterbach-Bahl et al. 2013; Poyda et al. 2016). Additionally, temporal fluctuations in soil moisture, as observed

during the water level increase in our study, are well documented for generating hotspots or triggering hot moments of N₂O production through denitrification (Butterbach-Bahl et al. 2013; Poyda et al. 2016). The cause for the higher N₂O emissions in *Carex* compared with intensive grassland remains uncertain, but clearly greater amounts of substrate for N₂O production must have been available in the *Carex* treatments. This can be attributed to reduced NO₃ uptake by *Carex* plants during the extended dormant period in winter compared with the intensive grassland vegetation. We can dismiss fertilizer contamination as a contributor to the high emissions from *Carex* treatments, as no fertilizer was applied in the previous year. Transplanting, however, might have influenced the availability of NO₃, as changes in site conditions may have accelerated peat mineralization. When we consider annual N₂O emissions without the pronounced peak fluxes, as these are not attributable to the overall experimental warming or rewetting treatment, the management shift toward *Carex* resulted in significantly lower total N₂O emissions compared to the intensive grassland (IDA 12.8 vs. CDA 6.3 kg N₂O ha⁻¹ year⁻¹).

Owing to the large N₂O emissions coupled with the substantial C export during the September harvest, the drained *Carex* treatment exhibited a GHG source with total emissions of 16.8 t CO₂-eq ha⁻¹ year⁻¹. The resulting emission is slightly lower than the mean value reported for extensive drained grassland in Germany of 22.5 t CO₂-eq ha⁻¹ year⁻¹ at a mean GWL of −0.29 m (Drösler et al. 2013). The subsequent reduction potential in this study amounted to −31.8 t CO₂-eq ha⁻¹ year⁻¹ or −65% (IDA vs. CDA). Total emissions shown in Fig. 4 align with current EFs and GHG balances for extensive grassland systems reported by Tiemeyer et al. (2020), although they fall towards the lower end of the range.

Rewetting

The successful rewetting was the basis for verifying the reduction potentials of wet cultivation of organic soils on net climate effects. The mean annual water level of −0.13 m in our rewetted areas achieved during the manipulation phase was close to the optimum of around −0.10 m proposed for reducing emissions from organic soils (e.g., Drösler et al. 2013; Tiemeyer et al. 2020; Evans et al. 2021). The absolute

difference in mean annual GWL between the drained and rewetted treatments was +0.17 m in the intensive grassland and +0.26 m in the *Carex* grassland. Rewetting resulted in a decrease in intensive grassland biomass production (IDA vs. IRA), while biomass production in the *Carex* grassland remained equal (CDA vs. CRA). Here, it was obvious that the intensive grassland plant community was not adapted to wet conditions while *Carex acutiformis* was well adapted to waterlogged conditions and has an optimum growth range over wider water level conditions (cf. Abel et al. 2013). The aerenchyma tissue provides an internal pathway for O₂ diffusion from the atmosphere to the roots oxygenating the belowground tissue and enabling survival under anoxic soil conditions after rewetting (Vroom et al. 2022). One option to preempt the negative yield development in rewetted intensive grasslands would be the adaptation of the species composition toward moisture tolerant intensive grassland species (e.g., *Festuca arundinacea* or *Phalaris arundinacea*) with desirable biomass yields and adjusted fertilization practices. The observed biomass yields in CRA are higher than the few published values for summer harvest of *C. acutiformis* ranging from 4.2 to 7.6 t ha⁻¹ given by Wichtmann et al. (2016) and 8.5 t ha⁻¹ reported for a GWL of +0.1 m by Günther et al. (2014). Results of the MOORuse project in the same study site (FSM) (data unpublished) revealed *C. acutiformis* biomass yields of 5.9 to 12.4 t ha⁻¹ under rewetted conditions (−0.05 to −0.13 m), 7.9 to 11.3 t ha⁻¹ under partly rewetted (−0.13 to −0.22 m), and 4.3 to 8.2 t ha⁻¹ under drained conditions (−0.27 to −0.45 m). Two further paludiculture sites in Bavaria established in the same project showed *C. acutiformis* biomass yields of 10.4 ± 2.7 and 11.6 ± 2.0 t ha⁻¹.

In terms of GHG emissions, rewetting of the intensive grassland (IRA) reduced the ecosystem respiration, photosynthesis (reflected in slightly reduced biomass yield) and NEE. This trend is in line with meta-studies by Blain et al. 2014 and Darusman et al. 2023 who report decreasing CO₂ emissions after rewetting interventions in various peatland ecosystems. The significant increase of CH₄ emissions was an expected result of anaerobic soil conditions under wetter conditions (e.g., Blain et al. 2014; Turetsky et al. 2014; Wen et al. 2018; Huth et al. 2020; Darusman et al. 2023). Compared to the implied national emission factor for German cropland and grassland

on organic soils the observed annual CH₄ emissions are lower but within the range of the national data set (Tiemeyer et al. 2020). The marginal decrease in N₂O fluxes was less than expected and reported in literature for rewetted conditions (e.g., Tiemeyer et al. 2020). However, the observed peak emissions that were related to freeze–thaw events and the start of water level manipulation, accounted for about half of the total N₂O budget. Our observations underline the importance of the time point of rewetting, as this can result in significant amounts of N₂O emissions (Brumme et al. 1999). This is particularly true when additional N₂O producing circumstances, such as freeze–thaw cycles, take place simultaneously as observed in the present study. Moreover, as the mean annual GWL of −0.13 m did not cause oxygen limitation in the upper soil layer, nitrification was not inhibited. Simultaneously, plant N demand was reduced at this treatment (IRA), apparent in the decreased yields, potentially providing more nitrate for microbial denitrification (cf. Offermanns et al. 2023). Furthermore, Brumme et al. (1999) state that small seasonal fluctuations of water level create aerobic and anaerobic microsites, which seem to be more important to N₂O emissions than the mean GWL if no year-round water saturation predominates. Without consideration of peak N₂O fluxes, rewetting significantly reduced annual N₂O emissions in all treatments. Still, the rewetted intensive grassland remained a net GHG source throughout the year with total emissions of 20.6 t CO₂-eq ha⁻¹ year⁻¹. Rewetting alone, while keeping the original intensive grassland vegetation, thus resulted in a distinct emission reduction of −27.8 t CO₂-eq ha⁻¹ year⁻¹ or 57%. This relative reduction compares well with values of −20 t CO₂-eq ha⁻¹ year⁻¹ after rewetting grassland on drained European temperate peat soils as given by the IPCC (2014), and with reductions of −26 t CO₂-eq ha⁻¹ year⁻¹ using German EFs (Tiemeyer et al. 2020). Net emissions are comparable to GHG emissions reported for extensive grassland systems under similar water level conditions in the study region (see Fig. 4).

While the reduction achieved from rewetting intensive grassland alone is promising from the mitigation perspective, a relevant aspect discussed by Kreyling et al. (2021) concerns the reestablishment of peatland ecosystem functions. The severe disturbance from drainage and agricultural practices of fen soils causes

degraded physical structures. Therefore, rewetting success may be additionally impaired, as extensive water table fluctuations can occur, which in turn stimulates discharge of nutrients after decades of overfertilization (Liu et al. 2019). The restoration of the self-regulation function—including the reestablishment of a C sink—as in natural peatlands, is thus questionable without further measures.

Creating a paludiculture system may be a promising solution, as we found that rewetting of the extensively managed *Carex* grassland (CRA) had a much greater desirable effect on all flux components. The high water level created ideal growth conditions for the wetland plant, which was reflected in the large GPP value, giving a considerable NEE uptake of $38 \text{ t CO}_2 \text{ ha}^{-1} \text{ year}^{-1}$. Despite four-times greater CH_4 emissions compared with drained conditions and a yield of $14.3 \pm 1.0 \text{ t DM ha}^{-1} \text{ year}^{-1}$ the system remained a GHG sink. The observed annual CH_4 emissions are in contrast to the implied national emission factor of $279 \text{ kg ha}^{-1} \text{ year}^{-1}$ given by Tiemeyer et al. (2020) for rewetted peatlands. The national data set for rewetted peatlands is aggregated from unutilized and wet peatlands, meaning areas for nature conservation or restored peatlands with higher groundwater levels ($< -0.1 \text{ m}$) compared to our rewetted treatments with -0.13 m . Günther et al. (2014) reported CH_4 emissions between 40 to $50 \text{ kg ha}^{-1} \text{ year}^{-1}$ for two managed *C. acutiformis* stands with mean groundwater levels of -0.03 to -0.01 m below the surface. In the previous year, the same treatments had significantly higher CH_4 emissions of up to $630 \text{ kg ha}^{-1} \text{ year}^{-1}$ but at a mean groundwater level of 0.10 m above the surface (Günther et al. 2014), demonstrating the risk of exponentially increasing CH_4 emissions with slightly increased water table, as also reported by Tiemeyer et al. (2020). Despite pronounced peak emissions during the freeze–thaw period, N_2O emissions in CRA were significantly reduced compared to the rewetted intensive grassland treatment as it is expected for rewetted organic soils (Joosten et al. 2015; Kandel et al. 2019; Tiemeyer et al. 2020). Total emissions in the first year after paludiculture establishment indicate a strong GHG sink of $-11.1 \text{ t CO}_2\text{-eq ha}^{-1} \text{ year}^{-1}$ (CRA). The resulting emission reduction potential in the *Carex* paludiculture amounted to $-59.5 \text{ t CO}_2\text{-eq ha}^{-1} \text{ year}^{-1}$ or -123% (CRA vs. IDA) and was far beyond the expected effects. While

we compare with relatively large emissions from our control site (IDA), the strong sink in CRA remains remarkable and lies well below the EFs for rewetted organic soils of 1.5 to $7 \text{ t CO}_2\text{-eq ha}^{-1} \text{ year}^{-1}$ (IPCC 2014) and 5.5 (range -5 to 22) $\text{t CO}_2\text{-eq ha}^{-1} \text{ year}^{-1}$ (Tiemeyer et al. 2020). The only published paludiculture simulation study by Günther et al. (2014) reports much larger emissions of $17.7 \text{ t CO}_2\text{-eq ha}^{-1} \text{ year}^{-1}$ for *C. acutiformis*. Here, the observed differences could be related to a distinctly higher GWL of $+0.1 \text{ m}$ and an earlier harvest event in July at a site with no harvest history. From a near natural fen site with small sedge reeds (including *Carex rostrata*) in Belarus, Minke et al. (2016) reported emissions of 0.5 to $5.3 \text{ t CO}_2\text{-eq ha}^{-1} \text{ year}^{-1}$ at GWL between -0.01 to $+0.10 \text{ m}$. We highlight that it cannot be completely ruled out that the transplanting of soil monoliths with adult *Carex* plants led to an increased biomass growth in the measurement year due to an adaptation to the new rewetted conditions. Once a new equilibrium was established, the observed strong CO_2 uptake could decrease. Hence, longer-term studies are necessary to prove the causation of the persistent strong sink function in the paludiculture. To verify the strong GHG sink function under rewetting, we included a *Carex* paludiculture dataset (Bockermann et al. in prep, MOORuse project results) for comparison in Fig. 4. The values correlate irrespective of the slightly differing management and rewetting history (planted *Carex* seedlings measured 2 to 5 years after establishment and rewetting, annual winter harvest), and different measurement years (2019–2021). Within this data set, it was found that the CO_2 uptake remained constant independent of the duration after establishment.

Climate warming effect on intensive drained grassland

We simulated an annual mean air temperature increase of $+0.9 \text{ }^\circ\text{C}$ in the drained intensive grassland (IDW) using passive warming. The achieved warming corresponds well to near-term warming scenarios of $+1.0$ to $+1.4 \text{ }^\circ\text{C}$ (0.8 to $2.2 \text{ }^\circ\text{C}$ depending on IPCC emission scenario) predicted for the study region until 2050 (LfU 2021). To a lesser extent, the moderate air warming significantly increased soil temperatures by $+0.7 \text{ }^\circ\text{C}$ at -2 cm soil depth in the drained intensive grassland. The observed effect of surface

warming on soil temperature corresponds well with most studies using OTCs (e.g., Chivers et al. 2009; Ward et al. 2013; Voigt et al. 2017; Oestmann et al. 2022), which is consistent with anticipated effects of climate warming.

As expected, warming increased the net emissions of all GHGs and stimulated biomass production in the drained intensive grassland (IDW), resulting in net annual GHG emissions of 66.9 t CO₂-eq ha⁻¹ year⁻¹ (+ 18.5 t CO₂-eq ha⁻¹ year⁻¹ or + 38% compared with IDA). Increased GHG emissions due to warming were also reported by Oestmann et al. (2022) for different bog sites in Germany. Net CO₂ emissions increased by 38%, resulting from 16% enhanced R_{eco} and a slightly less enhanced response of photosynthesis to warming (GPP increase of 8%). This relative increase in R_{eco} is in line with values given by Chivers et al. (2009) for an arctic fen site, whereas GPP increased by 16% negating the effect of climate warming in their study. Likewise, warming caused a 30% increase in biomass yield and an annual increase in CH₄ and N₂O fluxes of 185% and 12% respectively. From a global soil respiration database, Bond-Lamberty et al. (2018) conclude that warming leads to an increase in contribution of R_h relative to total soil respiration. Generally, increases in C and N fluxes from warmer organic soils can be attributed to a significant positive correlation between temperature and the increased availability of plant-derived labile substrates due to enhanced plant growth as reported by e.g., Wiesmeier et al. (2016) and Wilson et al. (2021). Increased amounts of easily decomposable organic substances can further cause a priming effect, i.e., the further acceleration of SOM decomposition (Kandel et al. 2013), enhancing R_h. As substrate becomes available, microbial activity intensifies with increasing temperature until it exceeds a certain threshold value, which limits the rate of enzymatic processes (Michaelis and Menten 1913; Lloyd and Taylor 1994; Schindlbacher et al. 2004). Leppelt et al. (2014) reported a positive correlation between N₂O emissions and temperature in a meta-study of European organic soils. They relate the effect to the pronounced sensitivity of denitrification to rising temperatures, whereby the Q₁₀ of denitrification even exceeds the Q₁₀ of soil CO₂ emissions (Schaufler et al. 2010; Butterbach-Bahl et al. 2013). Further, N₂O fluxes are indirectly affected by the temperature-induced respiratory depletion of

soil oxygen concentration (Butterbach-Bahl et al. 2013). Correspondingly, this warming-stimulated shift toward anaerobic soil conditions led to a greater relative increase in CH₄ (e.g., Bubier et al. 1995; Schrier-Uijl et al. 2010; Turetsky et al. 2014), which we also observed in all of our warming treatments. Hence, we can assume that the moderate warming in our experiment has led to an accelerated peat decay as postulated by e.g. Glatzel et al. (2006), stimulating all GHG emissions by enhancing plant growth and microbial processes. Regarding the 30% increase in biomass development observed under warming of the drained organic grassland (IDW), data on climate change effects on grassland on organic soils are not available for comparison. For European grasslands on mineral soils, model projections by Carozzi et al. (2022) suggest that a short to mid-term 1% increase in productivity will be followed by a significant long-term reduction of 7.7% as growing seasons will be shortened by rising temperatures exceeding the optimum photosynthetic window for many plant species.

Adaptation to warming

Warming of the ‘mitigation measures’ provided the opportunity to evaluate the climate change adaptation potential of the tested management options for organic soils. Both tested mitigation measures led to considerable net GHG reductions under warming. However, both systems resulted in suboptimal growth conditions in either rewetted intensive grassland communities (IRW) or drained *Carex* dominated stands (CDW). In the first year of warming, both systems exhibited slightly reduced vegetation growth and slightly increased total GHG emissions (Table 3; Fig. 4). Ward et al. (2013) and Oestmann et al. (2022) report similar responses of increased CO₂ and CH₄ fluxes to warming. While both studies found negligible effects on N₂O as their peatlands were near-natural nutrient-poor bogs, Rustad et al. (2001) found evidence for significantly increased N mineralization rates under warmed conditions in their meta-study on different ecosystems. In our case, the temperature-driven rise in peat soil mineralization intensified N₂O emissions, especially in the drained *Carex*, where the N surplus from mineralization coincided with the stage of plant aging in late summer when N demand is reduced. In the rewetted intensive grassland, it can be assumed that less NO₃ was available compared to

the IDW and CDW treatments due to the more anoxic soil conditions. Furthermore, the June harvest and plant regrowth resulted in an increased demand for N in summer, further reducing the mineral N content. We expect these developments to exacerbate under prolonged warming and predict a community composition shift after a transient species adaptation stage in the intensive grassland species.

The most apparent advantage of paludiculture establishment was the strong sink function, which resulted in an immediate mitigation effect. Surprisingly, the strong sink function was maintained under warming conditions, taking up $-13.1 \text{ t CO}_2\text{-eq ha}^{-1} \text{ year}^{-1}$ and amounted to total emission reductions of $-80 \text{ t CO}_2\text{-eq ha}^{-1} \text{ year}^{-1}$ compared with the drained intensive grassland under warming (IDA as our worst-case scenario). As observed in the IRW treatment, R_{eco} and GPP were also reduced at the CRW treatment compared to their ambient counterparts (IRA or CRA). Furthermore, both CO_2 flux components declined equally in the IRW treatment in response to warming ($R_{\text{eco}} - 6\%$, $\text{GPP} - 6.5\%$), whereas the CRW treatment exhibited an imbalanced decline with -23% in R_{eco} and -14% in GPP. In both the IRW and CRW treatments, the decline in GPP was also reflected in the reduced biomass yields of -3.5% and -11% respectively. This finding is contrary to our assumption, as we would expect a significant increase in R_{eco} due the stimulating effect of warming on peat mineralization as observed at the drained treatments. Nevertheless, the observed reduced amount of biomass also led to a reduced amount of autotrophic respiration (R_a). Assuming the same ratio of GPP to R_a for the plants in their respective ambient counterparts, R_h decreased significantly in the CRW treatment compared to the IRW treatment. The reason for this behavior is still unknown but one explanation could be significantly greater amounts of biomass developed in CRW compared to IRW, which likely led to greater amounts of root exudates (Wiesmeier et al. 2016; Wilson et al. 2021) favoring microbial oxygen consumption. In combination with warming, this restricted aerobic microbial activity in the upper few centimeters of the peat layer and reduced the overall R_h compared to the CRA treatment. The observed significantly higher CH_4 emissions, almost doubling those in the CRA treatment, could be an indicator for this theory.

In comparison to the other investigated mitigation measures, paludiculture appears to be the most resilient management option, offering the greatest sink even under climate warming. However, as mentioned above, these results represent only the initial response to altered conditions and longer-term studies are needed to prove the persistence of the strong observed sink function in the paludiculture under warming. One potential future drawback of paludicultures may be nutrient depletion over time, as export of nutrients (especially N-P-K) through biomass harvest is not compensated by fertilization. Long-term nutrient depletion can potentially limit GPP (Shaver et al. 2000) if the irrigation water does not cover the demand. Thus, there is a risk that the productivity of paludiculture will continue to decline under climate warming and negate the observed GHG sink function in the long term. Prudence is advisable when extrapolating our findings to other climate zones or differing initial soil conditions. Comparing field observations underline that climate warming affects different climate zones or regions differently (e.g., Lohila et al. 2010).

Conclusion

Germany is committed to achieving climate neutrality by 2045. Fulfilling this ambitious goal will require substantial emission reductions in all sectors. Organic soils are currently the largest single emission source within the LULUCF sector, therefore halting emissions from peatland soils should be a priority. Our results underline the need to act decisively on appropriate adaptation measures, as an increase of just 0.9°C in temperature—a moderate warming scenario predicted for the nearer future—was found to significantly enhance emissions from drained grassland on organic soils. This result further challenges the reliability of the current emission factors for estimates of GHG emissions in the near future. Despite large N_2O emissions observed in all treatments of this study, the general statements on mitigation and adaptation trends remain unaffected and reflect a conservative assessment.

Regarding mitigation measures, we confirm the high GHG reduction potentials for the two established measures of rewetting and management extensification. While we observed that warming led to an

absolute increase of emissions of both options, the relative mitigation potential remained. In this study, we found that the novel concept of paludiculture had the strongest emission reduction potential. Our results provide the first in situ field experimental evidence that an observed strong sink function for greenhouse gases could persist even under warming. This shows the potential of paludiculture to modify the impact of warming on ecosystem emissions and thus deliver a key measure for climate change adaptation on organic soils. Nevertheless, the current one-year study reflects only the initial response to altered conditions and longer-term studies are needed to prove the persistence of the strong observed sink function in the paludiculture.

Studies on adapted intensive grassland species composition with adjusted fertilization for wet cultivation could provide mitigation options for organic soils at sites where management extensification is not an option due to biomass quality requirements (e.g., fodder production for the bovine dairy industry). In terms of adaptation potential and resilience, additional studies assessing the long-term stability of paludiculture biomass development and persistence of the GHG sink strength will be meaningful. Lastly, testing climate change effects on different paludiculture species can contribute to robust emission factors and to informed decision making for implementation of larger scale paludiculture. This requires examining the various aspects of climate change (i.e., warming, CO₂ fertilization effect, changing precipitation and humidity pattern) through more holistically approached studies.

Acknowledgements We thank an anonymous referee for their careful revision of the manuscript and suggestions which improved the manuscript quality. We also thank Megan Seipp for proofreading the manuscript. Furthermore, we thank the landowner Josef Ziegltrum for providing the study site. This article is funded by the Open Access Publication Fund of Weihenstephan-Triesdorf University of Applied Sciences.

Author contributions TE and MD conceived the study. CB collected field data and performed all data analyses with contributions from TE. All authors discussed the results and implications. CB led writing of the manuscript with comments/edits from all authors.

Funding Open Access funding enabled and organized by Projekt DEAL. The research leading to these results received funding from Bavarian Ministry for Environment and Consumer Protection (Bayerisches Staatsministerium für Umwelt

und Verbraucherschutz, StMUV) under Grant Agreement No. 71F-U8729-2015/133-11-TLK01U-69371.

Data availability The datasets generated during and/or analyzed during the current study are not publicly available due to continued data analyses but are available from the corresponding author on reasonable request.

Declarations

Competing interests The authors have no relevant financial or non-financial interests to disclose.

Open Access This article is licensed under a Creative Commons Attribution 4.0 International License, which permits use, sharing, adaptation, distribution and reproduction in any medium or format, as long as you give appropriate credit to the original author(s) and the source, provide a link to the Creative Commons licence, and indicate if changes were made. The images or other third party material in this article are included in the article's Creative Commons licence, unless indicated otherwise in a credit line to the material. If material is not included in the article's Creative Commons licence and your intended use is not permitted by statutory regulation or exceeds the permitted use, you will need to obtain permission directly from the copyright holder. To view a copy of this licence, visit <http://creativecommons.org/licenses/by/4.0/>.

References

- Abel S, Couwenberg J, Dahms T, Joosten H (2013) The Database of Potential Paludiculture Plants (DPPP) and results for Western Pomerania. *Plant Ecol Divers* 130(3–4):219–228
- Baird AJ, Comas X, Slater LD, Belyea LR, Reeve AS (2009) Understanding carbon cycling in Northern Peatlands: recent developments and future prospects. In: Baird AJ, Belyea LR, Comas X, Reeve AS, Slater LD (eds) *Carbon cycling in northern Peatlands*, vol 184. Geophysical monograph series. American Geophysical Union, Washington
- Bechtold M, Tiemeyer B, Laggner A, Leppelt T, Frahm E, Belting S (2014) Largescale regionalization of water table depth in peatlands optimized for greenhouse gas emission upscaling. *Hydrol Earth Syst Sci* 18:3319–3339. <https://doi.org/10.5194/hess-18-3319-2014>
- Blain D, Murdiyarso D, Couwenberg J, Nagata O, Renou-Wilson F, Sirin A, Strack M, Tuittila E-S, Wilson D (2014) Rewetted organic soils. In: Hiraishi T, Krug T, Tanabe K, Srivastava N, Baasansuren J, Fukuda M, Troxler TG (eds) 2013 Supplement to the 2006 IPCC guidelines for national greenhouse gas inventories: wetlands. IPCC, Geneva
- BMEL (2020) Federal Ministry of Food and Agriculture: agriculture and climate change mitigation. <https://www.bmel.de/EN/topics/farming/climate-stewardship/agriculture-climate-change-mitigation.html>

- BMUV (2021) National Peatland Protection Strategy. Federal Ministry for the Environment, Nature Conservation, Nuclear Safety and Consumer Protection. <https://www.bmuv.de/en/download/the-national-peatland-protection-strategy>
- Bond-Lamberty M, Gough CM, Vargas R (2018) Globally rising soil heterotrophic respiration over recent decades. *Nature* 560(7716):80–83. <https://doi.org/10.1038/s41586-018-0358-x>
- Brumme R, Borken W, Finke S (1999) Hierarchical control on nitrous oxide emission in forest ecosystems. *Global Biogeochem Cycles* 13(4):1137–1148
- Bubier JL, Moore TR, Bellisario L, Comer NT, Crill PM (1995) Ecological controls on methane emissions from a northern peatland complex in the zone of discontinuous permafrost, Manitoba, Canada. *Glob Biogeochem Cycles* 9(4):455–470
- Butterbach-Bahl K, Baggs EM, Dannenmann M, Kiese R, Zechmeister-Boltenstern S (2013) Nitrous oxide emissions from soils: how well do we understand the processes and their controls? *Philos Trans R Soc Lond B Biol Sci* 368(1621):20130122. <https://doi.org/10.1098/rstb.2013.0122>
- Carozzi M, Martin R, Klumpp K, Massad RS (2022) Effects of climate change in European croplands and grasslands: productivity, greenhouse gas balance and soil carbon storage. *Biogeosciences* 19(12):3021–3050. <https://doi.org/10.5194/bg-19-3021-2022>
- Chivers MR, Turetsky MR, Waddington JM, Harden JW, McGuire AD (2009) Effects of experimental water table and temperature manipulations on ecosystem CO₂ fluxes in an Alaskan rich fen. *Ecosystems* 12:1329–1342. <https://doi.org/10.1007/s10021-009-9292-y>
- Crawley MJ (2007) *The R Book*. Wiley, Hoboken. <https://doi.org/10.1002/9780470515075>
- Darusman T, Murdiyarso D, Impron AI (2023) Effect of rewetting degraded peatlands on carbon fluxes: a meta-analysis. *Mitig Adapt Strateg Glob Chang* 28(3):10. <https://doi.org/10.1007/s11027-023-10046-9>
- Drösler M (2005) Trace gas exchange and climatic relevance of bog ecosystems, Southern Germany. Dissertation, Technical University Munich
- Drösler M, Freibauer A, Christensen T, Friborg T (2008) Observation and status of peatland greenhouse gas emission in Europe. In: Dolman H, Valentini R, Freibauer A (eds) *The Continental-scale greenhouse gas balance of Europe*. Springer, New York
- Drösler M, Adelmann W, Augustin J et al (2013) Klimaschutz durch Moorschutz. Schlussbericht des BMBF-Vorhabens: Klimaschutz - Moornutzungsstrategien 2006–2010 Report No. FKZ 01LS05046 – 01LS05051
- DWD Climate Data Center (CDC) (2023) Historische monatliche Stationsbeobachtungen (Temperatur, Druck, Niederschlag, Sonnenscheindauer, etc.) für Deutschland. Version v21.3, 2021 [Database]. https://opendata.dwd.de/climate_environment/CDC/observations_germany/climate/monthly/kl/historical/. Accessed 10 Oct 2023
- Eberl (2016) *Aufbau eines Informationssystems Freisinger Moos*. Bachelor thesis, University of Applied Sciences Weihenstephan-Triesdorf
- EC (2021) Communication from the Commission to the European Parliament, the Council, the European Economic and Social Committee and the Committee of the Regions. Forging a climate-resilient Europe – the new EU Strategy on Adaptation to Climate Change. COM/2021/82 final. <https://eur-lex.europa.eu/legal-content/EN/TXT/?uri=COM:2021:82:FIN#footnoteref2>. Accessed 10 Mar 2023
- Eickenscheidt T (2015) Assessment and modeling of greenhouse gas emissions (CO₂, CH₄, N₂O) from different land-use types and management practices on drained fen peatlands and associated organic soils—case study Freisinger Moos. Dissertation, Technical University Munich
- Eickenscheidt T, Freibauer A, Heinichen J, Augustin J, Drösler M (2014) Short-term effects of biogas digestate and cattle slurry application on greenhouse gas emissions affected by N availability from grasslands on drained fen peatlands and associated organic soils. *Biogeosciences* 11(22):6187–6207. <https://doi.org/10.5194/bg-11-6187-2014>
- Eickenscheidt T, Heinichen J, Drösler M (2015) The greenhouse gas balance of a drained fen peatland is mainly controlled by land-use rather than soil organic carbon content. *Biogeosciences* 12(17):5161–5184. <https://doi.org/10.5194/bg-12-5161-2015>
- Elsgaard L, Görres CM, Hoffmann CC, Blicher-Mathiesen G, Schelde K, Petersen SO (2012) Net ecosystem exchange of CO₂ and carbon balance for eight temperate organic soils under agricultural management. *Agric Ecosyst Environ* 162:52–67. <https://doi.org/10.1016/j.agee.2012.09.001>
- Estop-Aragónés C, Blodau C (2012) Effects of experimental drying intensity and duration on respiration and methane production recovery in fen peat incubations. *Soil Biol Biochem* 47:1–9. <https://doi.org/10.1016/j.soilbio.2011.12.008>
- Evans CD, Peacock M, Baird AJ, Artz RRE, Burden A, Callaghan N, Chapman PJ, Cooper HM, Coyle M, Craig E, Cumming A, Dixon S, Gauci V, Grayson RP, Helfter C, Heppell CM, Holden J, Jones DL, Kaduk J et al (2021) Overriding water table control on managed peatland greenhouse gas emissions. *Nature* 593:548–552. <https://doi.org/10.1038/s41586-021-03523-1>
- Falge E, Baldocchi D, Olson R, Anthoni P, Aubinet M, Bernhofer C, Burba G, Ceulemans R, Clement R, Dolman H, Granier A, Gross P, Grünwald T, Hollinger D, Jensen N-O, Katul G, Keronen P, Kowalski A, Lai CT, Law BE, Wofsy S (2001) Gap filling strategies for defensible annual sums of net ecosystem exchange. *Agric For Meteorol* 107(1):43–69. [https://doi.org/10.1016/S0168-1923\(00\)00225-2](https://doi.org/10.1016/S0168-1923(00)00225-2)
- Fan N, Reichstein M, Koirala S, Ahrens B, Mahecha MD, Carvalhais N (2022) Global apparent temperature sensitivity of terrestrial carbon turnover modulated by hydrometeorological factors. *Nat Geosci* 15(12):989–994. <https://doi.org/10.1038/s41561-022-01074-2>
- Flessa H, Wild U, Klemisch M, Pfadenhauer J (1998) Nitrous oxide and methane fluxes from organic soils under agriculture. *Eur J Soil Sci* 49:327–335
- Freeman BWJ, Evans CD, Musarika S, Morrison R, Newman TR, Page SE, Wiggs GFS, Bell NGA, Styles D, Wen Y, Chadwick DR, Jones DL (2022) Responsible agriculture

- must adapt to the wetland character of mid-latitude peatlands. *Glob Chang Biol* 28(12):3795–3811. <https://doi.org/10.1111/gcb.16152>
- Fuß R, Hueppi R, Pedersen AR (2020) gasfluxes: greenhouse gas flux calculation from chamber measurements (0.4–4). <https://CRAN.R-project.org/package=gasfluxes>
- Glatzel S, Lemke S, Gerold G (2006) Short-term effects of an exceptionally hot and dry summer on decomposition of surface peat in a restored temperate bog. *Eur J Soil Biol* 42(4):219–229. <https://doi.org/10.1016/j.ejsobi.2006.03.003>
- Gong Y, Wu J, Vogt J, Ma W (2020) Greenhouse gas emissions from peatlands under manipulated warming, nitrogen addition, and vegetation composition change: a review and data synthesis. *Environ Rev* 28(4):428–437. <https://doi.org/10.1139/er-2019-0064>
- Günther A, Huth V, Jurasinski G, Glatzel S (2014) The effect of biomass harvesting on greenhouse gas emissions from a rewetted temperate fen. *Glob Chang Biol Bioenergy* 7:1092–1106
- Günther A, Barthelmes A, Huth V, Joosten H, Jurasinski G, Koebsch F, Couwenberg J (2020) Prompt rewetting of drained peatlands reduces climate warming despite methane emissions. *Nat Commun* 11(1):1644. <https://doi.org/10.1038/s41467-020-15499-z>
- Hahn-Schöfl M, Zak D, Minke M, Gelbrecht J, Augustin J, Freibauer A (2011) Organic sediment formed during inundation of a degraded fen grassland emits large fluxes of CH₄ and CO₂. *Biogeosciences* 8(6):1539–1550. <https://doi.org/10.5194/bg-8-1539-2011>
- Hamidov A, Helming K, Bellocchi G, Bojar W, Dalgaard T, Ghaley BB, Hoffmann C, Holman I, Holzkämper A, Krzeminska D, Kvaernø SH, Lehtonen H, Niedrist G, Øygarden L, Reidsma P, Roggero PP, Rusu T, Santos C, Seddaiu G, Skarbøvik E, Ventrella D, Żarski J, Schönhart M (2018) Impacts of climate change adaptation options on soil functions: a review of European case-studies. *Land Degrad Dev* 29(8):2378–2389. <https://doi.org/10.1002/ldr.3006>
- Hothorn T, Bretz F, Westfall P, Heiberger RM, Schuetzenmeister A, Scheibe S (2021) multcomp: simultaneous inference in general parametric models (1.4–17). <https://CRAN.R-project.org/package=multcomp>
- Huang Y, Ciais P, Luo Y, Zhu D, Wang Y, Qiu C, Goll DS, Guenet B, Makowski D, De Graaf I, Leifeld J, Kwon MJ, Hu J, Qu L (2021) Tradeoff of CO₂ and CH₄ emissions from global peatlands under water-table drawdown. *Nat Clim Chang* 11(7):618–622. <https://doi.org/10.1038/s41558-021-01059-w>
- Huth V, Günther A, Bartel A, Hofer B, Jacobs O, Jantz M, Meister M, Rosinski E, Urich T, Weil M, Zak D, Jurasinski G (2020) Topsoil removal reduced in-situ methane emissions in a temperate rewetted bog grassland by a hundredfold. *Sci Total Environ* 721:137763. <https://doi.org/10.1016/j.scitotenv.2020.137763>
- IPCC (2014) In: Hiraishi T, Krug T, Tanabe K, Srivastava N, Baasansuren J, Fukuda M, Troxler TG (eds) 2013 Supplement to the 2006 IPCC Guidelines for National Greenhouse Gas Inventories: wetlands. IPCC, Geneva
- IPCC (2018) In: Masson-Delmotte V, Zhai P, Pörtner H-O, Roberts D, Skea J, Shukla PR, Pirani A, Moufouma-Okia W, Péan C, Pidcock R, Connors SL, Matthews JBR, Chen Y, Zhou X, Gomis MI, Lonnoy E, Maycock T, Tignor M, Waterfield T (eds) Global warming of 15°C. An IPCC Special Report on the impacts of global warming of 1.5°C above pre-industrial levels and related global greenhouse gas emission pathways, in the context of strengthening the global response to the threat of climate change, sustainable development and efforts to eradicate poverty. Cambridge University Press, Cambridge
- IPCC (2021) In: Masson-Delmotte V, Zhai P, Pirani A, Connors SL, Péan C, Berger S, Caud N, Chen Y, Goldfarb L, Gomis MI, Huang M, Leitzell K, Lonnoy E, Matthews JBR, Maycock TK, Waterfield T, Yelekçi O, Yu R, Zhou B (eds) Climate Change 2021: The Physical Science Basis. Contribution of Working Group I to the Sixth Assessment Report of the Intergovernmental Panel on Climate Change. Cambridge University Press, Cambridge. <https://doi.org/10.1017/9781009157896>
- IPCC (2022) In: Pörtner H-O, Roberts DC, Tignor T, Poloczanska ES, Mintenbeck K, Alegria A, Craig M, Langsdorf S, Löschke S, Möller V, Okem A, Rama B (eds) Climate Change 2022: impacts, adaptation and vulnerability. Contribution of Working Group II to the Sixth Assessment Report of the Intergovernmental Panel on Climate Change. Cambridge University Press, Cambridge. <https://doi.org/10.1017/9781009325844>
- IUSS Working Group WRB (2015) World Reference Base for Soil Resources 2014, update 2015 International soil classification system for naming soils and creating legends for soil maps. FAO, Rome
- Joosten H, Gaudig G, Krawczynski R, Tanneberger F, Wichmann S, Wichtmann W (2015) Managing soil carbon in Europe: Paludicultures as a new perspective for peatlands. In Banwart SA, Noellemeier E, Milne E (eds) Soil carbon: science, management and policy for multiple benefits. CABI, Wallingford, 1. Aufl, S. 297–306. <https://doi.org/10.1079/9781780645322.0297>
- Jungkunst HF, Flessa H, Scherber C, Fiedler S (2008) Groundwater level controls CO₂, N₂O and CH₄ fluxes of three different hydromorphic soil types of a temperate forest ecosystem. *Soil Biol Biochem* 40(8):2047–2054. <https://doi.org/10.1016/j.soilbio.2008.04.015>
- Jurasinski G, Koebsch F, Guenther A, Beetz S (2014) flux: flux rate calculation from dynamic closed chamber measurements (0.3–0). <https://CRAN.R-project.org/package=flux>
- Kandel TP, Elsgaard L, Karki S, Lærke PE (2013) Biomass yield and greenhouse gas emissions from a drained fen peatland cultivated with reed canary grass under different harvest and fertilizer regimes. *Bioenerg Res* 6:883–895. <https://doi.org/10.1007/s12155-013-9316-5>
- Kandel TP, Karki S, Elsgaard L, Lærke PE (2019) Fertilizer-induced fluxes dominate annual N₂O emissions from a nitrogen-rich temperate fen rewetted for paludiculture. *Nutr Cycl Agroecosyst* 115(1):57–67. <https://doi.org/10.1007/s10705-019-10012-5>
- Kasimir-Klemedtsson A, Klemedtsson L, Berglund K, Martikainen P, Silvola J, Oenema O (1997) Greenhouse gas emissions from farmed organic soils: a review. *Soil Use Manag* 13:245–250
- Kreyling J, Tanneberger F, Jansen F, van der Linden S, Aggenbach C, Blüml V, Couwenberg J, Emsens WJ,

- Joosten H, Klimkowska A, Kotowski W, Kozub L, Lennartz B, Liczner Y, Liu H, Michaelis D, Oehmke C, Parakenings K, Pleyl E et al (2021) Rewetting does not return drained fen peatlands to their old selves. *Nat Commun* 12(1):5693. <https://doi.org/10.1038/s41467-021-25619-y>
- Lahtinen L, Mattila T, Myllyviita T, Seppälä J, Vasander H (2022) Effects of paludiculture products on reducing greenhouse gas emissions from agricultural peatlands. *Ecol Eng* 175:106502. <https://doi.org/10.1016/j.ecoleng.2021.106502>
- Laine AM, Mäkiranta P, Laiho R, Mehtätalo L, Penttilä T, Korrensalo A, Minkkinen K, Fritze H, Tuittila E (2019) Warming impacts on boreal fen CO₂ exchange under wet and dry conditions. *Glob Chang Biol* 25(6):1995–2008. <https://doi.org/10.1111/gcb.14617>
- Leiber-Sauheitl K, Fuß R, Voigt C, Freibauer A (2014) High CO₂ fluxes from grassland on histic Gleysol along soil carbon and drainage gradients. *Biogeosciences* 11(3):749–761. <https://doi.org/10.5194/bg-11-749-2014>
- Lenth RV, Buerkner P, Herve M, Love J, Miguez F, Riebl, H, Singmann H (2021) emmeans: Estimated Marginal Means, aka Least-Squares Means (1.7.1-1). <https://CRAN.R-project.org/package=emmeans>
- Leppelt T, Dechow R, Gebbert S, Freibauer A, Lohila A, Augustin J, Drösler M, Fiedler S, Glatzel S, Höper H, Järveoja J, Lærke PE, Maljanen M, Mander Ü, Mäkiranta P, Minkkinen K, Ojanen P, Regina K, Strömberg M (2014) Nitrous oxide emission budgets and land-use-driven hotspots for organic soils in Europe. *Biogeosciences* 11(23):6595–6612. <https://doi.org/10.5194/bg-11-6595-2014>
- LFU (Bayerisches Landesamt für Umwelt) (2021) Bayerns Klima im Wandel: Klimaregion Südbayerisches Hügelland [Infoblatt]. Bayerisches Landesamt für Umwelt. www.lfu.bayern.de
- Liu H, Zak D, Rezanezhad F, Lennartz B (2019) Soil degradation determines release of nitrous oxide and dissolved organic carbon from peatlands. *Environ Res Lett* 14(9):094009. <https://doi.org/10.1088/1748-9326/ab3947>
- Livingston GP, Hutchinson GL (1995) Enclosure-based measurement of trace gas exchange: application and sources of error. In: Biogenic trace gases: measuring emissions from soil and water. Blackwell, Cambridge, pp 14–50
- Lloyd J, Taylor JA (1994) On the temperature dependence of soil respiration. *Funct Ecol* 8(3):315–323. <https://doi.org/10.2307/2389824>
- Lohila A, Minkkinen K, Laine J, Savolainen I, Tuovinen J-P, Korhonen L, Laurila T, Tietäväinen H, Laaksonen A (2010) Forestation of boreal peatlands: impacts of changing albedo and greenhouse gas fluxes on radiative forcing. *JGR Biogeosciences* 115(G4):G04011. <https://doi.org/10.1029/2010JG001327>
- Loisel J, Gallego-Sala A (2022) Ecological resilience of restored peatlands to climate change. *Commun Earth Environ* 3(1):208. <https://doi.org/10.1038/s43247-022-00547-x>
- Loisel J, Gallego-Sala AV, Amesbury MJ, Magnan G, Anshari G, Beilman DW, Benavides JC, Blewett J, Camill P, Charman DJ, Chawchai S, Hedgpeth A, Kleinen T, Korhola A, Large D, Mansilla CA, Müller J, Van Belen S, West JB et al (2021) Expert assessment of future vulnerability of the global peatland carbon sink. *Nat Clim Change* 11(1):70–77. <https://doi.org/10.1038/s41558-020-00944-0>
- Marion GM, Henry GHR, Freckman DW, Johnstone J, Jones G, Jones MH, Lévesque E, Molau U, Mølgaard P, Parsons AN, Svoboda J, Virginia RA (1997) Open-top designs for manipulating field temperature in high-latitude ecosystems. *Glob Change Biol* 3(S1):20–32. <https://doi.org/10.1111/j.1365-2486.1997.gcb136.x>
- Metzger C, Jansson P-E, Lohila A, Aurela M, Eickenscheidt T, Beletti-Marchesini L, Dinsmore KJ, Drewer J, van Huissteden J, Drösler M (2015) CO₂ fluxes and ecosystem dynamics at five European treeless peatlands—merging data and process oriented modelling. *Biogeosciences* 12:125–146. <https://doi.org/10.5194/bg-12-125-2015>
- Michaelis L, Menten ML (1913) Die Kinetik der Invertinwirkung. *Biochemische Zeitschrift* 49:333–369. urn:nbn:de:hebis:30-1090119
- Minke M, Augustin J, Burlo A, Yarmashuk T, Chuvashova H, Thiele A, Freibauer A, Tikhonov V, Hoffmann M (2016) Water level, vegetation composition, and plant productivity explain greenhouse gas fluxes in temperate cutover fens after inundation. *Biogeosciences* 13(13):3945–3970. <https://doi.org/10.5194/bg-13-3945-2016>
- Myhre G, Shindell D, Bréon F-M, Collins W, Fuglestad J, Huang J, Koch D, Lamarque J-F, Lee D, Mendoza B, Nakajima T, Robock A, Stephens G, Takemura T, Zhang H (2013) In: Stocker TF, Qin D, Plattner G-K, Tignor M, Allen SK, Boschung J, Nauels A, Xia Y, Bex V, Midgley PM (eds) Anthropogenic and Natural Radiative Forcing. In: Climate Change 2013: the physical science basis. Contribution of Working Group I to the Fifth Assessment Report of the Intergovernmental Panel on Climate Change. Cambridge University Press, Cambridge
- Nugent KA, Strachan IB, Roulet NT, Strack M, Froliking S, Helbig M (2019) Prompt active restoration of peatlands substantially reduces climate impact. *Environ Res Lett* 14(12):124030. <https://doi.org/10.1088/1748-9326/ab56e6>
- Oestmann J, Dettmann U, Düvel D, Tiemeyer B (2022) Experimental warming increased greenhouse gas emissions of a near-natural peatland and *Sphagnum* farming sites. *Plant Soil* 480:85–104. <https://doi.org/10.1007/s11104-022-05561-8>
- Offermanns L, Tiemeyer B, Dettmann U, Rüffer J, Düvel D, Vogel I, Brümmer C (2023) High greenhouse gas emissions after grassland renewal on bog peat soil. *Agric For Meteorol* 331:109309. <https://doi.org/10.1016/j.agrfor.2023.109309>
- Pearson M, Penttilä T, Harjunpää L, Laiho R, Laine J, Sarjala T, Silvan K, Silvan N (2015) Effects of temperature rise and water-table-level drawdown on greenhouse gas fluxes of boreal sedge fens. *Boreal Environ Res* 20:489–505
- Pérez-Priego O, López-Ballesteros A, Sánchez-Cañete EP, Serano-Ortiz P, Kutzbach L, Domingo F, Eugster W, Kowalski AS (2015) Analysing uncertainties in the calculation of fluxes using whole-plant chambers: random and systematic errors. *Plant Soil* 393(1):229–244

- Petersen SO, Hoffmann CC, Schäfer C-M, Bilcher-Mathiesen G, Elsgaard L, Kristensen K, Larsen SE, Torp SB, Greve MH (2012) Annual emissions of CH₄ and N₂O, and ecosystem respiration, from eight organic soils in Western Denmark managed by agriculture. *Biogeosciences* 9:403–422
- Pinheiro J, Bates D, R Core Team (2023) *Nlme: linear and nonlinear mixed effects models*. R package version 3.1-162. <https://CRAN.R-project.org/package=nlme>
- Poyda A, Reinsch T, Kluß C, Loges R, Taube F (2016) Greenhouse gas emissions from fen soils used for forage production in northern Germany. *Biogeosciences* 13:5221–5244. <https://doi.org/10.5194/bg-13-5221-2016>
- R Core Team (2022) *R: a language and environment for statistical computing*. R Foundation for Statistical Computing, Vienna. <https://www.R-project.org/>
- Renou-Wilson F, Barry C, Müller C, Wilson D (2014) The impacts of drainage, nutrient status and management practice on the full carbon balance of grasslands on organic soils in a maritime temperate zone. *Biogeosciences* 11(16):4361–4379. <https://doi.org/10.5194/bg-11-4361-2014>
- Rustad L, Campbell J, Marion G, Norby R, Mitchell M, Hartley A, Cornelissen J, Gurevitch J (2001) A meta-analysis of the response of soil respiration, net nitrogen mineralization, and aboveground plant growth to experimental ecosystem warming. *Oecologia* 126(4):543–562. <https://doi.org/10.1007/s004420000544>
- Salimi S, Berggren M, Scholz M (2021) Response of the peatland carbon dioxide sink function to future climate change scenarios and water level management. *Glob Chang Biol* 27(20):5154–5168. <https://doi.org/10.1111/gcb.15753>
- Schauffler G, Kitzler B, Schindlbacher A, Skiba U, Sutton MA, Zechmeister-Boltenstern S (2010) Greenhouse gas emissions from European soils under different land use: effects of soil moisture and temperature. *Eur J Soil Sci* 61:683–696. <https://doi.org/10.1111/j.1365-2389.2010.01277.x>
- Schindlbacher A, Zechmeister-Boltenstern S, Butterbach-Bahl K (2004) Effects of soil moisture and temperature on NO, NO₂, and N₂O emissions from European forest soils. *J Geophys Res Atmos* 109(D17):2004JD004590. <https://doi.org/10.1029/2004JD004590>
- Schrier-Uijl AP, Kroon PS, Hensen A, Leffelaar PA, Berendse F, Veenendaal EM (2010) Comparison of chamber and eddy covariance-based CO₂ and CH₄ emission estimates in a heterogeneous grass ecosystem on peat. *Agric For Meteorol* 150(6):825–831. <https://doi.org/10.1016/j.agrfor.2009.11.007>
- Shaver GR, Canadell J, Chapin FS, Gurevitch J, Harte J, Henry G, Ineson P, Jonasson S, Melillo J, Pitelka L, Rustad L (2000) Global warming and terrestrial ecosystems: a conceptual framework for analysis. *Bioscience* 50(10):871. [https://doi.org/10.1641/0006-3568\(2000\)050\[0871:GWATEAJ2.0.CO;2](https://doi.org/10.1641/0006-3568(2000)050[0871:GWATEAJ2.0.CO;2)
- Tanneberger F, Appulo L, Ewert S, Lakner S, Ó Brolcháin N, Peters J, Wichtmann W (2021) The power of nature-based solutions: how peatlands can help us to achieve key EU sustainability objectives. *Adv Sustain Syst* 5(1):2000146. <https://doi.org/10.1002/adsu.202000146>
- Tanneberger F, Birr F, Couwenberg J, Kaiser M, Luthardt V, Neger M, Pfister S, Oppermann R, Zeitz J, Beyer C, Van Der Linden S, Wichtmann W, Närmann F (2022) Saving soil carbon, greenhouse gas emissions, biodiversity and the economy: Paludiculture as sustainable land use option in German fen peatlands. *Reg Environ Change* 22(2):69. <https://doi.org/10.1007/s10113-022-01900-8>
- Tiemeyer B, Albiac Borraz E, Augustin J, Bechtold M, Beet S, Beyer C, Drösler M, Ebli M, Eickenscheidt T, Fiedler S, Förster C, Freibauer A, Giebel M, Glatzel S, Heinichen J, Hoffmann M, Höper H, Jurasinski G, Leiber-Sauheitl K et al (2016) High emissions of greenhouse gases from grasslands on peat and other organic soils. *Glob Chang Biol* 22(12):4134–4149. <https://doi.org/10.1111/gcb.13303>
- Tiemeyer B, Freibauer A, Borraz EA, Augustin J, Bechtold M, Beet S, Beyer C, Ebli M, Eickenscheidt T, Fiedler S, Förster C, Gensior A, Giebel M, Glatzel S, Heinichen J, Hoffmann M, Höper H, Jurasinski G, Laggenner A et al (2020) A new methodology for organic soils in national greenhouse gas inventories: data synthesis, derivation and application. *Ecol Indic* 109:105838. <https://doi.org/10.1016/j.ecolind.2019.105838>
- Turetsky MR, Kotowska A, Bubier J, Dise NB, Crill P, Hornibrook ERC, Minkinen K, Moore TR, Myers-Smith IH, Nykänen H, Olefeldt D, Rinne J, Saarnio S, Shurpali N, Tuittila E-S, Waddington JM, White JR, Wickland KP, Wilmking M (2014) A synthesis of methane emissions from 71 northern, temperate, and subtropical wetlands. *Glob Chang Biol* 20(7):2183–2197. <https://doi.org/10.1111/gcb.12580>
- UBA (Federal Environment Agency) (2023) Submission under the United Nations Framework Convention on Climate Change and the Kyoto Protocol 2023: National Inventory Report for the German Greenhouse Gas Invent 1990–2021. Umweltbundesamt. <http://www.umweltbundesamt.de/publikationen>
- Updegraff K, Bridgman SD, Pastor J, Weishampel PA, Harth C (2001) Response of CO₂ and CH₄ emissions in peatlands to warming and water table manipulation. *Ecol Appl* 11(2):311–326. <https://doi.org/10.2307/3060891>
- Van Beek CL, Pleijter M, Jacobs CMJ, Velthof GL, van Groenigen JW, Kuikman PJ (2010) Emissions of N₂O from fertilized and grazed grassland on organic soil in relation to groundwater level. *Nutr Cycl Agroecosyst* 86:331–340
- Van Beek CL, Pleijter M, Kuikman PJ (2011) Nitrous oxide emissions from fertilized and unfertilized grasslands on peat soil. *Nutr Cycl Agroecosyst* 89:453–461
- Velthof GL, Brader AB, Oenema O (1996) Seasonal variations in nitrous oxide losses from managed grasslands in the Netherlands. *Plant Soil* 181:263–274
- Voigt C, Lamprecht RE, Maruschak ME, Lind SE, Novakovskiy A, Aurela M, Martikainen PJ, Biasi C (2017) Warming of subarctic tundra increases emissions of all three important greenhouse gases—carbon dioxide, methane, and nitrous oxide. *Glob Chang Biol* 23(8):3121–3138. <https://doi.org/10.1111/gcb.13563>

- Vroom RJE, Geurts JJM, Nouta R, Borst ACW, Lamers LPM, Fritz C (2022) Paludiculture crops and nitrogen kick-start ecosystem service provisioning in rewetted peat soils. *Plant Soil* 474(1–2):337–354. <https://doi.org/10.1007/s11104-022-05339-y>
- Waldo NB, Hunt BK, Fadely EC, Moran JJ, Neumann RB (2019) Plant root exudates increase methane emissions through direct and indirect pathways. *Biogeochemistry* 145(1–2):213–234. <https://doi.org/10.1007/s10533-019-00600-6>
- Ward SE, Ostle NJ, Oakley S, Quirk H, Henrys PA, Bardget RD (2013) Warming effects on greenhouse gas fluxes in peatlands are modulated by vegetation composition. *Ecol Lett* 16:1285–1293. <https://doi.org/10.1111/ele.12167>
- Wen X, Unger V, Jurasinski G, Koebsch F, Horn F, Rehder G, Sachs T, Zak D, Lischeid G, Knorr K-H, Böttcher ME, Winkel M, Bodelier PLE, Liebner S (2018) Predominance of methanogens over methanotrophs in rewetted fens characterized by high methane emissions. *Biogeosciences* 15:6519–6536. <https://doi.org/10.5194/bg-15-6519-2018>
- Whalen SC (2005) Biogeochemistry of methane exchange between natural wetlands and the atmosphere. *Environ Eng Sci* 22(1):73–94
- Wichtmann W, Schröder C, Joosten H (2016) Paludiculture—productive use of wet peatlands. Schweizerbart Science Publishers, Stuttgart
- Wiesmeier M, Poeplau C, Sierra CA, Maier H, Frühauf C, Hübner R, Kühnel A, Spörlein P, Geuß U, Hangen E, Schilling B, von Lützow M, Kögel-Knabner I (2016) Projected loss of soil organic carbon in temperate agricultural soils in the 21st century: effects of climate change and carbon input trends. *Sci Rep* 6:32525. <https://doi.org/10.1038/srep32525>
- Wilson D, Blain D, Couwenberg J (2016) Greenhouse gas emission factors associated with rewetting of organic soils. *Mires Peat* 17(4):1–28. <https://doi.org/10.19189/MaP.2016.OMB.222>
- Wilson RM, Tfaily MM, Kolton M, Johnston ER, Petro C, Zelman CA, Hanson PJ, Heyman HM, Kyle JE, Hoyt DW, Eder EK, Purvine SO, Kolka RK, Sebestyen SD, Griffiths NA, Schadt CW, Keller JK, Bridgman SD, Chanton JP, Kostka JE (2021) Soil metabolome response to whole-ecosystem warming at the Spruce and Peatland responses under changing environments experiment. *PNAS* 118(25):e2004192118. <https://doi.org/10.1073/pnas.2004192118>
- Wittnebel M, Frank S, Tiemeyer B (2023) Aktualisierte Kulisse organischer Böden in Deutschland. Johann Heinrich von Thünen-Institut, Braunschweig, Thünen Working Paper 212. <https://doi.org/10.3220/WP1683180852000>
- Wunsch A, Liesch T, Broda S (2022) Deep learning shows declining groundwater levels in Germany until 2100 due to climate change. *Nat Commun* 13(1):1221. <https://doi.org/10.1038/s41467-022-28770-2>
- Zuur AF, Ieno EN, Walker N, Saveliev AA, Smith GM (2009) Mixed effects models and extensions in ecology with R. Springer, New York. <https://doi.org/10.1007/978-0-387-87458-6>

Publisher's Note Springer Nature remains neutral with regard to jurisdictional claims in published maps and institutional affiliations.